N O T I C E

THIS DOCUMENT HAS BEEN REPRODUCED FROM MICROFICHE. ALTHOUGH IT IS RECOGNIZED THAT CERTAIN PORTIONS ARE ILLEGIBLE, IT IS BEING RELEASED IN THE INTEREST OF MAKING AVAILABLE AS MUCH INFORMATION AS POSSIBLE

JOINT INSTITUTE FOR AERONAUTICS AND ACOUSTICS
STANFORD UNIVERSITY

Semi-Annual Progress Report

July 1, 1980 - December 31, 1980

on

APPLICATION OF HOLOGRAPHY TO THE STUDY OF HELICOPTER ROTOR FLOW FIELDS

NASA-Ames Grant No. NAG 2-45

Submitted to the

National Aeronautics and Space Administration
Ames Research Center
Moffett Field, California 94035

Y. H. Yu - Technical Officer

by the

Joint Institute for Aeronautics and Acoustics
Department of Aeronautics and Astronautics
Stanford, University
Stanford, California 94035

Donald Baganoff - Principal Investigator

Tad McGeer - Research Assistant

May 29, 1981

ABSTRACT

This paper considers the feasibility of an experiment which is intended to measure the density field about a model Helicopter Rotor using holographic interferometry. The experiment is studied through a numerical simulation which we describe after a brief review of the measurement technique itself. We then present the data generated by this simulation, and assess the prospects both for determining the density field from these data, and for actually obtaining such data in practice. A few significant problems which may be expected to arise are indicated and discussed.

INTRODUCTION

The U.S. Army Aeromechanics Laboratory at NASA-Ames is currently planning an experiment to measure the density field about a helicopter rotor using holographic interferometry. This measurement is to be made in the Laboratory's Anechoic Hover Chamber using a 1/7-scale UH-1 rotor. The scale of this test, and the character of the flow field to be measured, make this probably the most ambitious application of holographic interferometry ever contemplated: consequently, it is by no means obvious that the application will be successful. Since there is a risk involved, some indication that the technique will work would obviously be desirable before committing substantial resources to the project. We at Stanford have therefore undertaken an analysis of the feasibility of this experiment. Here we report the results that we have obtained to date.

We begin by reviewing the experimental procedure. The first step in making the measurement involves recording a set of projections of the flow field. In our case, a projection is a profile of integrals of refractive index (which is linearly related to density) along rays through the flow field. Thus, the value of the projection at point (ξ,z) and orientation θ, as shown in figure 1, is

$$\varphi(\xi,\theta,z) = \int_s n(x,y,z)\,ds$$

where $n(x,y,z)$ is the refractive index at (x,y,z), and s is the path of the light ray incident at (ξ,z). The path s is in general curved as a result of refraction, although in many practical cases its curvature may be neglected.

Holographic interferometry is used to obtain the set of projections as follows. First, a reference hologram of the undisturbed field viewed at angle θ is recorded. Then, a second hologram of the disturbed field is made using the same optical system. Simultaneous holographic playback of the two produces a pattern of interference fringes. The fringe shift at a point (ξ,z) on the pattern is directly proportional to the difference between the optical pathlengths to that point through the disturbed and undisturbed fields. Thus, if the fringe shift at (ξ,z) is N, then the change in pathlength is $N\lambda$ where λ is the wavelength of the probing light. Since the undisturbed refractive index field is known a priori, this interference pattern determines the projection of the disturbed field at angle θ. The same procedure is repeated for a number of viewing angles to compose a complete set of data.

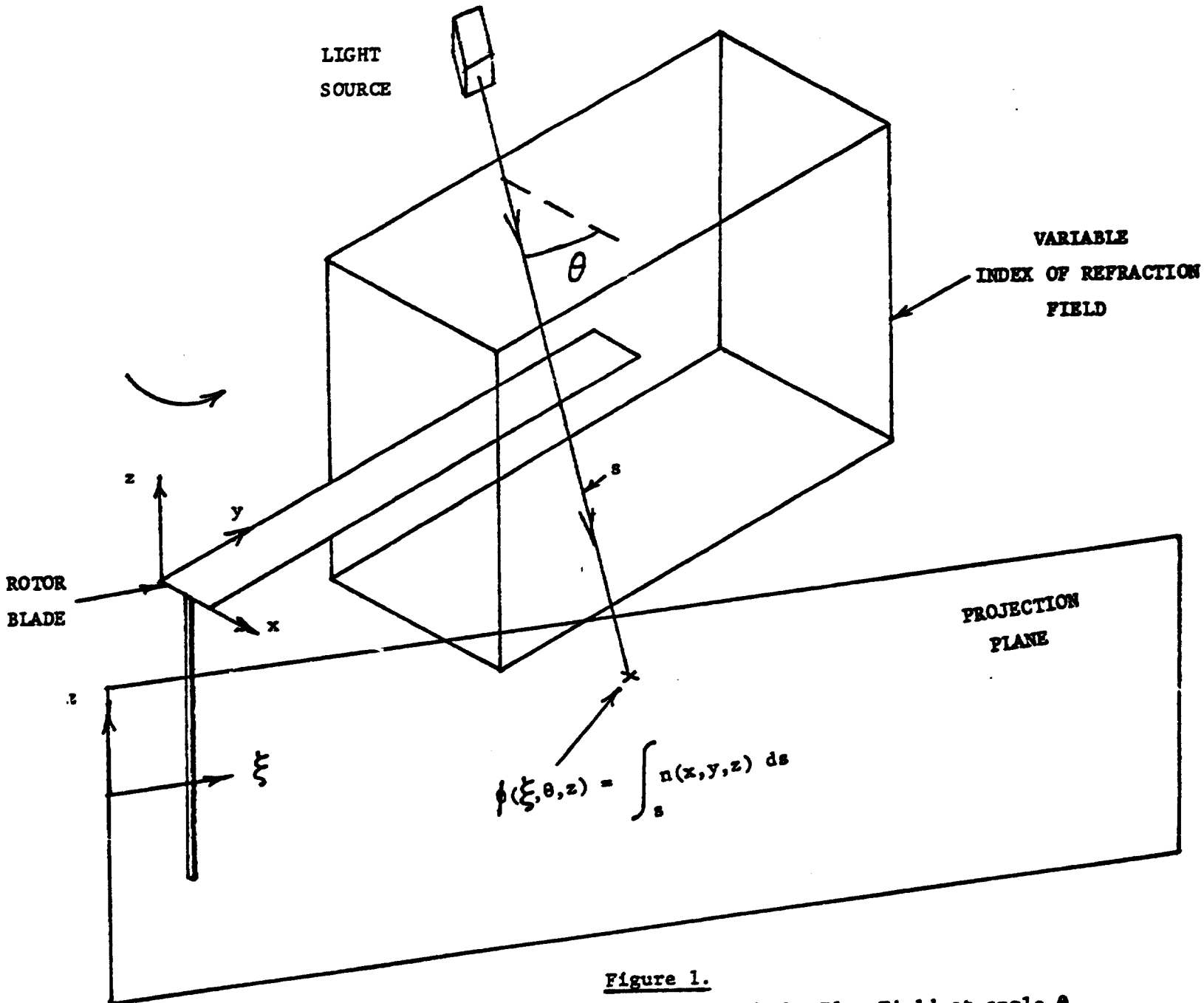

Figure 1.
Projection of the Flow Field at angle θ.

With these data in hand, the object refractive index field may be computed using techniques of reconstruction from projections. A variety of methods have been formulated for performing this calculation, so that reconstruction in cases where first, a complete set of projections spanning 180 degrees in Θ is available, and second, the probing rays are straight lines, is a matter of routine. If either of these conditions is violated, however, the reconstruction problem is considerably more difficult. Unfortunately, refraction will not be small in our case; we shall discuss the consequences of this presently.

For the moment, we simply point out that the experiment will involve two steps, both of which must be performed effectively in order to produce an acceptable result. First, the interferometric measurement must make available projection data which are sufficiently complete and noise-free to effect reconstruction. Second, the reconstruction method must yield a solution having satisfactory accuracy and resolution.

THE ASSESSMENT PROCEDURE

We have chosen to assess each of these steps through a numerical simulation of the proposed experiment. The input to the simulation is a solution for the velocity field about the tip of the rotor blade - the region of interest to us - computed by Caradonna [1]. We calculate the corresponding refractive index field, and determine its projections by numerical integration. These data may then be used as input to a reconstruction routine, whose solution may be compared to the original input field. This comparison allows us to quantitatively assess the results, which is the great advantage of simulation. Thus, we can determine precisely the effects of a number of different factors which we may introduce, including noise of various types and magnitudes, variations in data sampling rates, different reconstruction algorithms, and so forth.

In particular, we can expect to obtain the following information from the simulation:

1. An impression of the general character of the projections.

2. An estimate of the magnitude of the fringe shifts to be expected.

3. A measure of refraction effects.

4. Minimum sampling rates in ξ, z, and Θ which will permit acceptable reconstruction.

5. Identification of the most effective reconstruction method for the field of interest.

We shall now discuss the simulation and the results obtained thus far.

THE INPUT VELOCITY FIELD

Let us begin by reviewing the input data. We have used Caradonna's solution for a case typical of those to be studied, that of zero rotor thrust and a blade tip mach number of 0.9. This solution is given as values of the chordwise velocity component on a grid of 50 points chordwise by 62 radially by 32 vertically, spanning the volume

$-5.8\ c < x < 10.2\ c$ chordwise, where c is the blade chord.
$0.75\ R < y < 1.75\ R$ radially, where R is the blade radius.
$0.015\ c < z < 22.6\ c$ vertically.

Most of the significantly disturbed region of the flow field is within this volume.

The sensitivity of the interferometric measurement increases with the scale of the disturbed field, so we must be specific about its dimensions in doing the simulation. We have used the chord and radius of the blade to be tested:

$c = 3$ in. $= 7.62$ cm.
$R = 41$ in. $= 1.04$ m.

The corresponding refractive index field

For the simulation we need the refractive index distribution, which is obtained from the velocity data by first calculating the density at each point, and then expressing this as a refractive index. The first step involves a form of Bernoulli's equation which applies for compressible flow that is steady with respect to a rotating (i.e. blade fixed) reference frame. This is presented by Caradonna [1]:

$$a^2 = a_0^2 + (\gamma-1)\left[\Omega r \cdot V - \frac{V^2}{2}\right]$$

where a is the speed of sound, and V is the fluid vector velocity measured with respect to fixed space. The flow is sufficiently isentropic that the speed of sound may be eliminated in favour of density. Upon doing so we obtain

$$\frac{\rho}{\rho_0} = \left[1 + \frac{(\gamma-1)}{a_0^2}\left(\Omega r U_\theta - \left(U_r^2 + \frac{U_\theta^2 + U_z^2}{2}\right)\right)\right]^{\frac{1}{\gamma-1}}$$

U_r^2 and U_z^2 are small compared to the other terms, and may be neglected. We are therefore left with

$$\frac{\rho}{\rho_0} = \left[1 + \frac{(\gamma-1)}{a_0^2}\left(\Omega r U_\theta - \frac{U_\theta^2}{2}\right)\right]^{\frac{1}{\gamma-1}}$$

(ρ / ρ_0) is directly related to the change in refractive index between disturbed and undisturbed states by the Gladstone-Dale formula

$$n - n_0 = K_{\rho_0}\left(\frac{\rho}{\rho_0} - 1\right)$$

The Gladstone-Dale constant K is a function of the refracting medium and, weakly, of the wavelength of the probing light. We intend to use a ruby laser, whose wavelength is 694.3 nm., in the experiment; the Gladstone-Dale constant for air at this wavelength is 2.25x10-4 m^3/Kg. The reference density and speed of sound must also be specified before we can compute the refractive index; we have used standard sea level values, namely

$$\rho_0 = 1.23 \ kg/m^3$$

$$a_0 = 340.3 \ m/s$$

Direct application of these formulae allows us to convert from U_∞, the chordwise velocity, to $(n-n_0)$, the change in index of refraction between the disturbed an undisturbed fields, at each point of Caradonna's solution. Contour plots of several horizontal planes through this $(n-n_0)$ field are presented in figures 2-6, while larger scale views of the region near the blade tip are shown in figures 7-11. It is appropriate for us to leave the refractive index in this form, rather than to compute the disturbed field explicitly, since, as we shall see, each interferogram may be regarded as a projection of the $(n-n_0)$ field.

We should say a few words at this point about the quality of these input data. Obviously, if they were known to be correct, then we would not be contemplating a difficult experimental measurement of them! In fact, while hot-wire data agree well with the numerical solution near the blade, they differ significantly in the region off the blade tip. The latter region is of particular interest in the planned investigation since it contains a propagating shock wave.

However, despite these discrepancies, the fidelity of the solution is sufficient for our purposes. For example, while the propagating shock is not faithfully reproduced by the numerical solution, some of its characteristics are evident in the band which may be seen extending off the blade tip in the figures. We require no more than such general similarity to assess the feasibility of the experiment.

CALCULATION OF FRINGE PATTERNS

We shall discuss the refractive index field in more detail presently in considering the relationship between the field and its projections. For the moment, we shall concentrate upon calculation of the projections themselves.

We have assumed that refraction is negligible in making these calculations. (This is a very desirable situation but we cannot justify the assumption solely on the basis of optimism; rather, we shall assess its validity after the fact.) Thus we have treated the probing rays as straight. Furthermore, we have considered them to be parallel to the rotor disc, consistent with our plan to use a horizontal beam in the actual experiment.

In this refractionless limit, two substantial simplifications

emerge. First, since rays do not cross horizontal planes through the field, each plane may be treated independently both in calculating the projections and in performing the reconstruction. Second, since each ray of probing light traverses the same path through both the undisturbed and the object fields, a holographic interferogram will record the projection of the $(n-n_o)$ field. That is, the fringe shift recorded at a point (ξ,z) on an interferogram exposed at viewing angle Θ will be

$$N(\xi,\Theta,z) = \frac{\Delta\varphi(\xi,\Theta,z)}{\lambda}$$

$$= \frac{1}{\lambda}\left(\varphi(\xi,\Theta,z) - \varphi_o(\xi,\Theta,z)\right)$$

$$= \frac{1}{\lambda}\left(\int_S n(x,y,z)\,ds - \int_S n_o(x,y,z)\,ds\right)$$

$$= \frac{1}{\lambda}\int_S (n-n_o)\,ds$$

We can therefore produce a computer-generated interferogram for the viewing angle Θ by numerically line integrating through horizontal planes of our $(n-n_o)$ field to a grid of points (ξ,z). A set of interferograms can be composed by repeating these calculations for a number of viewing angles.

Actual interferograms would of course differ from these computer generated versions, since the refractive index field used as input to our calculations is neither completely accurate nor does it encompass the entire region of disturbance - it does not include the inner 75% of the blade. But we have previously concluded that the first limitation - inaccuracy of the numerical solution - is tolerable, since only approximate information on the object field is needed for our feasibility study. For the same reason, we can also do without data on the relatively small disturbances over the inner portion of the blade. This is best appreciated by examining the fringe patterns themselves, to which we now turn.

THE CALCULATED FRINGE PATTERNS

We have calculated projections for a variety of viewing angles between -75 and +90 degrees. Figure 12 povides a guide to these, showing the orientation of each projection with respect to the blade. ξ, the horizontal coordinate in the projection plane, is measured from the projected rotor hub; the convention is indicated in the figure. Figures 13-22 show the projections themselves. In that we have plotted these by drawing the loci of half-integer fringes ($N = \pm 0.5, \pm 1.5, \pm 2.5, \ldots$) and leaving the intevening spaces blank, these figures represent so-called 'infinite-fringe' interferograms of the flow field.

All of the projections plotted in this way are quite striking

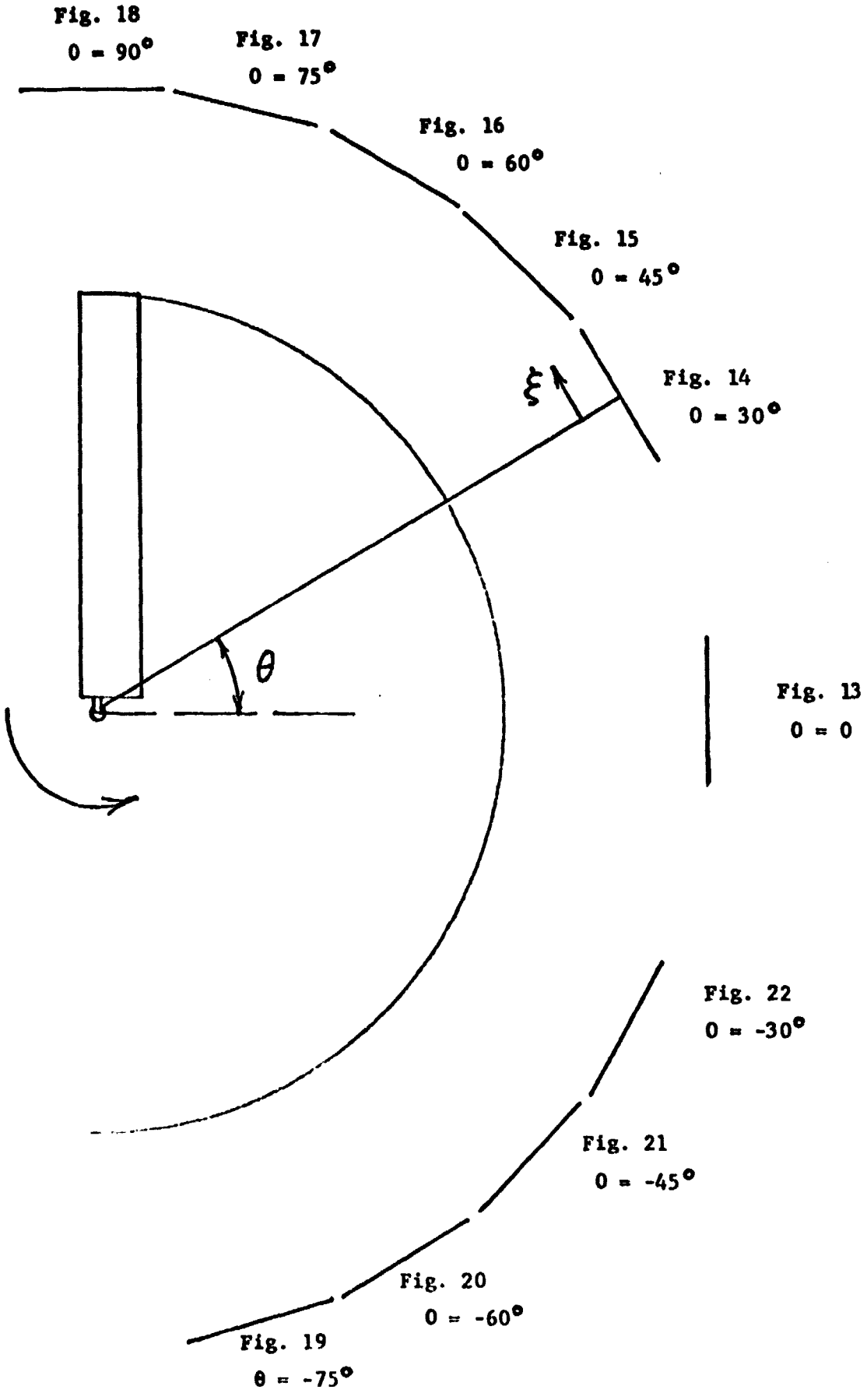

Figure 12. A guide to the plotted projections.

and some have a certain aesthetic appeal. But perhaps the most impressive of all is the chordwise projection (figure 13). For, when plotted as an infinite fringe interference pattern, it is completely blank. Nowhere, apparently, do the optical pathlengths through the undisturbed and object fields differ by as much as one-half wavelength - 350 nanometers. An actual interferogram would therefore consist only of diffuse gray bands and would have very little contrast.

This result may be understood by considering the plots of the $(n-n_0)$ fields in figures 2-11. Note that the region of significant disturbance is thin in the chordwise direction, extending little beyond the leading and trailing edges of the blade. Thus, disturbances over only a short segment of any line through the field contribute to the projection integral. Moreover, the sign of the disturbance oscillates over this short segment from positive ahead of the blade, to negative in the region of reduced pressure above it, and back to positive behind the trailing edge. Therefore, disturbances over the middle of the line segment tend to cancel those at either end, and as a result the net line integral is very small.

At the other extreme, we have the radial (90°) projection. The disturbed region is long in this direction, and most of the disturbance along any given line through the field is of the same sign. Thus large fringe shifts are produced - a bright fringe of order +25 lies just ahead of and above the projected leading edge ($\xi=0$), while one of order -25 lies slightly above the 1/4-chord of the blade. Integration over the inner 75% of the blade, which has been excluded from our calculations, would tend to increase these magnitudes.

There is, then, a large gradient in fringe shift across the radial projection. This is troublesome. An immedeately apparent problem is that individual fringes become indistinct in such a strong gradient; thus in order to accurately determine the fringe order over this rather important region of the projection one would somehow have to either reduce the sensitivity of the measurement or improve the clarity of the fringe patterns. A more fundamental problem is that such closely spaced fringes indicate that refraction is most certainly not negligible, as we can demonstrate by the following calculation. Vest [2] suggests the criterion that if the quantity

$$\frac{\lambda L}{d_f^2}$$

exceeds about 0.3, then refraction should be taken into account. Here d_f is the fringe spacing, and L is the distance between imaging lenses in the optical system. In our case, we have

$$L \sim 30\,m = 3\times10^{4}\,mm.$$

Therefore, according to this criterion, refraction will be significant if

$$d_f^2 < \frac{(5.943\times10^{-4}\,mm)(3\times10^{4}\,mm)}{0.3}$$

$$d_f < \sim 7\,mm.$$

Fortunately, while this condition is violated by about 1 order of magnitude in the radial projection, it is at least marginally satisfied at lower angles. Consider, for example, the projection at +75 degrees. Rays traversing the field at this angle are nearly tangent to the band of disturbance extending off the blade. We would expect this fairly long transit through a band of significant variation in the refractive index to produce a large fringe shift, and indeed this is the case. The fringe order varies from -17 to +3.5 across the projection. (These values would not change very much if the field over the inner 75% of the disc were included, since rays within the band off the blade have only short segments within the disturbed part of that field.) The minimum fringe spacing in this projection is 3-4 mm., which may be considered marginally satisfactory with respect to the refraction criterion.

As the projection angle is reduced further from chordwise, the fringe spacing continues to increase, and the magnitude of the fringe shift correspondingly decreases. This is a consequence of both shortened pathlengths through the disturbed region and oscillations in the sign of $(n-n_o)$ along these paths. Similar behavior is evident for angles between -75 degrees and 0; however, the fringe pattern for any given negative projection angle is less rich than that for its positive counterpart, since rays inclined at negative angles travel across rather than along the disturbed band off the blade tip. An important feature here is the pronounced variation in the nature of the fringe patterns with projection angle. This characteristic of the $(n-n_o)$ field bears significantly upon the field of view required for reconstruction, as we shall see.

THE FEASIBILITY OF RECONSTRUCTION

Having calculated and examined the projections of the refractive index field, we can now address the following question: can this field be reconstructed with satisfactory accuracy and resolution using input data from these projections? Although we have not yet attempted a reconstruction, we can indicate some of the factors which will affect its feasibility.

The theory of reconstruction from projections affords an analytical solution provided that two conditions are satisfied:

1. Complete knowledge of the projection, $\beta(\zeta,z,\theta)$, over a 180 degree range of viewing angles is available.

2. Refraction is negligible.

In practice, the analytical solution is adapted to accept discrete data. Reconstruction algoriths differ in their input requirements - some can accept input points spaced non-uniformly in ζ and θ, for example - but a guide is provided by the sampling theorem. This theorem indicates that input data points should be separated by no more than twice the maximum spatial frequency of the disturbance field in the direction perpendicular to the projection; otherwise aliasing will produce artifacts in the reconstruction. This is a lower limit, however, since redundant

data are always required to suppress noise.

Now, in sampling fringe patterns, one cannot determine precisely the fringe order at each of a set of uniformly spaced points. One can only determine whether a selected point lies within either a bright (integer-order) or a dark (half-integer order) fringe, and the resolution of a direct measurement is therefore limited to $\pm 1/4$ fringe shift. For example, one would assign the value zero to each point on a fringe pattern such as that shown for the chordwise viewing direction, although the actual value varies between ± 0.2.

There are techniques whereby sharper resolution can be obtained. The simplest way would be by graphical interpolation between the centrelines of bright and dark fringes; this technique would be applicable to the richer fringe patterns obtained at higher projection angles. Another method would involve the use of so-called 'finite-fringe' interferograms. Thus, one introduces an artificial pathlength gradient across the projection between holographic exposures of the reference and object fields. Then if the object field contained no disturbance, holographic playback of the two exposures would produce an interference pattern consisting of equally spaced parallel fringes. The actual disturbance field will displace these fringes, and the pathlength data is extracted by measuring their displacement. Again, the sampling rate is determined by the fringe spacing, but by using this technique that spacing can be reduced arbitrarily - at least to the point where adjacent fringes become indistinct.

While it is possible, then, to resolve fringe shifts to higher accuracy than $\pm 1/2$, this level of accuracy should be quite acceptable for input to a reconstruction routine. Moreover, higher accuracy would perhaps be unjustified in view of the noise level to be expected.

Field of view

Of course, the field of interest to us contains shock waves, which are very high frequency structures. Therefore, we can anticipate that quite high sampling rates in both ξ and θ will be required in projections near tangent to the shocks - those within about 20 degrees of spanwise - to obtain an alias-free reconstruction having reasonable spatial resolution.

This suggests that the present apparatus will place a very severe limitation on the quality of the reconstruction, for it has a restricted field of view which will prevent recording of projections near spanwise. This restriction can be appreciated by considering figure 23. The probing light passes across the test chamber, from one side of the rotor disc to the other. If only one blade's disturbance field is to be included in the reconstruction process (the alternative would obviously increase the experimental and computational burden enormously), then each ray which traverses one blade's field must not intersect that of the other blade. Since the region of significant disturbance extends outward from about halfway along the blade, and about 1.5 chords out from the leading and trailing edges (the former of which is itself about 1/4 chord ahead of the

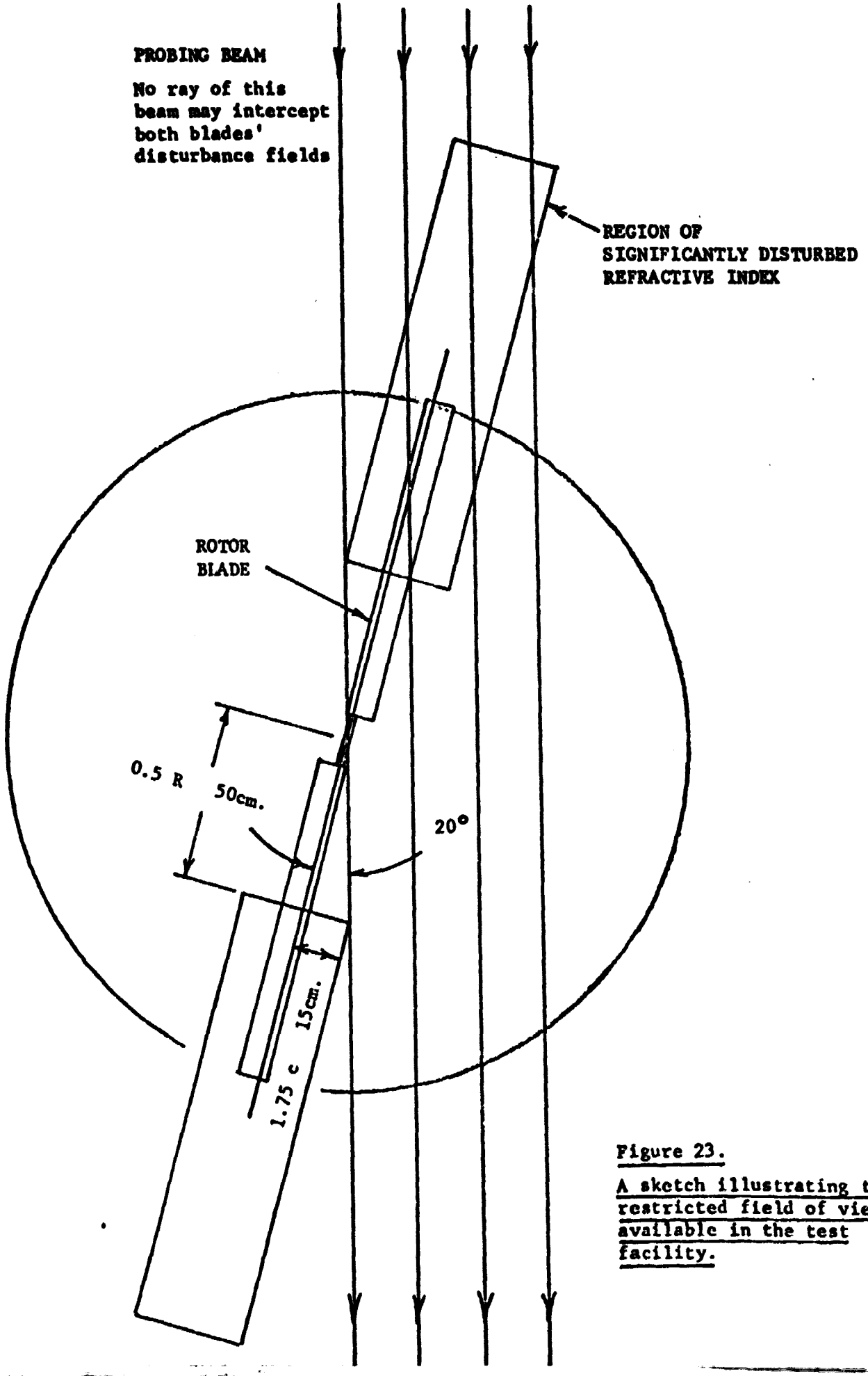

Figure 23.

A sketch illustrating the restricted field of view available in the test facility.

diameter of the rotor disc) this restriction excludes angles within about 20 degrees of spanwise.

While this limitation of the field of view to about 140 degrees can be tolerated if the object field is 'roundish' (if not completely axisymmetric) - provided that clean projection data is available and that care is used in the reconstruction - for our field, whose character varies drastically with viewing angle, a full 180 degree field of view will likely be required. This could only be obtained with an experimental arrangement different from that presently contemplated. Three possible schemes are as follows:

First, we might place a mirror on the rotor hub to reflect the beam away from the second blade. However, the problems of mounting a mirror of the necessary size on the hub while meeting stringent requirements for optical quality and stability are formidable; therefore this scheme would probably not be practicable.

Second, we might rearrange the optical system so that the probing beam was parallel to a vertical plane rather than the rotor disc. We could measure only that portion of the disturbance field outside the disc using this arrangement, since blockage by an opaque blade, or refraction by a transparent blade, would preclude recording of projections within the diameter of the disc. This scheme would have additional disadvantages in that it would mandate extensive modifications to the test chamber, and the entire optical system would have to be moved to record each new projection. The results would probably not justify the effort involved.

A third possibility would be to use a single-bladed rotor. Such a rotor would place quite a strain on the dynamic components of the rotor system, and might require some modifications to the affected hardware. While we would prefer to avoid the consequent effort and expense of implementing this scheme, no practical alternative which would satisfy the field of view requirement is evident.

Refraction

Another significant problem which we have mentioned earlier is refraction. Since refraction is not negligible in projections within about 25 degrees of spanwise, the refractionless limit cannot be assumed in performing the reconstruction. The question is rather whether a first-order correction will take this effect into account satisfactorily, or, instead, a full-blown iterative reconstruction will be necessary. A discouraging sign is that both the horizontal and the vertical fringe spacings in the radial projection violate the criterion for negligible refraction. This implies that horizontal planes cannot be treated independently in the reconstruction, and that a three-dimensional scheme will be necessary. Reconstruction in such circumstances is by no means a closed problem and a satisfactory solution consequently cannot be assured; in any case, the difficulties of developing a reconstruction scheme and of implementing it would be substantial.

NOISE IN THE EXPERIMENTAL DATA

For the moment let us assume that a practical reconstruction scheme can be developed, and consider the question of whether sufficiently noise-free input data for such a routine can actually be obtained in practice. Actually, noise may well make these data rather difficult to measure. We can illustrate this by a simple calculation.

Variations in temperature between recordings of the reference and object exposures will be one source of random noise. Let us estimate the temperature stability which would have to be maintained in order to measure the same fringe shifts that we have calculated in our simulation. Assume that, between exposures of the reference and object fields, the temperature changes from To to T. Then the fringe shift produced by this temperature change alone is given by

$$\Delta N = \frac{L}{\lambda}\left(n(T) - n(T_0)\right) \approx \frac{L}{\lambda}\frac{dn}{dT}(T - T_0)$$

where L is the physical pathlength in the optical system. dn/dT may be found using the equation of state and the Gladstone-Dale formula. We have that

$$\frac{dn}{dT} = \frac{dn}{d\rho}\frac{d\rho}{dT}$$

From the equation of state,

$$\frac{d\rho}{dT} = \frac{-p}{RT^2} = \frac{-\rho}{T}$$

and, from the Gladstone-Dale formula,

$$\frac{dn}{d\rho} = K = 2.25 \times 10^{-4}\ m^3/kg \qquad @ \quad T = 290^\circ K, \quad \lambda = 694.3\ nm$$

Thus,

$$\frac{dn}{dT} = -\frac{K\rho}{T}$$

and

$$\Delta N = \frac{L}{\lambda}\left(-\frac{K\rho}{T}\right)(T - T_0)$$

$$= -1.35 \times L \times \Delta T$$

for L in metres and dT in degrees Kelvin. In our case, L is about 20 m. If we require that temperature variations produce fringe shifts of no more than 1/2, then we must maintain constant temperature to within

$$\Delta T = \frac{0.5^{\circ}}{(1.35)(20)} \approx 0.02^{\circ}K$$

Now, a uniform temperature change between exposures of the reference and object fields of this magnitude, or any other for that matter, could be detected easily and then removed from the measurement. However, random variations in temperature across the field cannot be dealt with so easily. While random variations would have to be of larger amplitude to produce a 1/2-fringe shift noise level in the projections, such variations are not inconceivable since air is continuously pumped from outdoors into the Anechoic Room, and around inside the facility, while the experiment is in progress. This effect must therefore be of some concern.

Nor is this the only source of noise. Besides additional sources of random noise, there is the problem of unsteadiness in the flow field. All projections of such a large field cannot be measured simultaneously; in fact, since the region of significant disturbance is wider in some directions than the aperture of the optical system, even single projections must be composites. In order to compose a projection the optics must be moved with respect to the rotor, while to assemble a set of projections exposures must be made with the rotor at various different azimuths. Consequently, since there is both a periodic variation in the disturbance with azimuth due to the non-axisymmetry of the Anechoic Room, and random unsteadiness, different parts of some projections, and projections taken at different angles, will in fact be projections of somewhat different flow fields. In this circumstance the best that one could hope to obtain from the reconstruction would be a rather blurred image of the flow field. High frequency components, particularly shock waves, would tend to be washed out of the image; since these features are of primary interest, the utility of the results would therefore be much reduced.

SUMMARY

Through our simulation and analysis of the planned experiment we have identified a number of factors which may be expected to complicate the holographic measurement or limit the quality of the density field reconstruction. These include:

1. The restricted field of view of the present apparatus.
2. Refraction in projections near spanwise.
3. Random noise.
4. Unsteadiness in the flow field.

We intend to do a number of reconstructions from our simulated projections which will provide further information on the effects of these factors. The cases to be considered are as follows:

1. Reconstruction with a full 180 degrees of noise-free projection data.

2. Reconstruction with the field of view limited to 140 degrees.

3. Reconstruction with a 180 degree field of view and artificially generated random noise superimposed upon the projection data.

4. Reconstruction with both superimposed noise and a restricted field of view.

Comparison of the reconstructions calculated in the last three cases with that of the first case will allow quantitative definition of the limitations imposed by noise and a restricted field of view. We shall present these results in a later report.

REFERENCES

1. Frank Caradonna, The Transonic Flow about a Helicopter Rotor, Ph.D. Dissertation, Stanford University, 1978.

2. Charles Vest, Holographic Interferometry, Wiley, 1979.

Figure 2.

$(n - n_o)$ FIELD IN PLANE 0.11 cm. ABOVE THE BLADE

contour interval = 20×10^{-6}

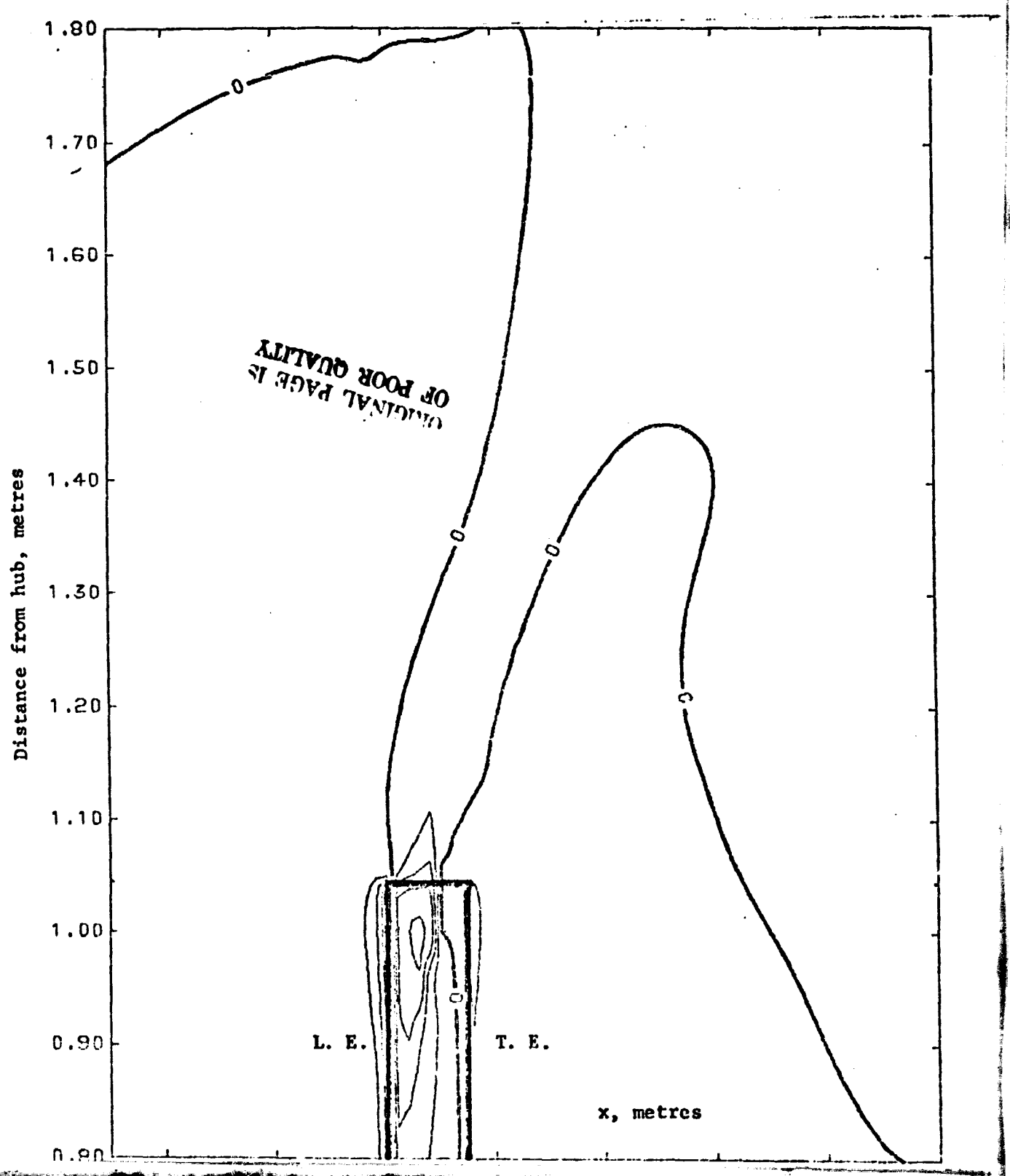

Figure 3.

$(n - n_o)$ FIELD IN PLANE 2.2 cm. ABOVE THE BLADE

contour interval = 10×10^{-6}

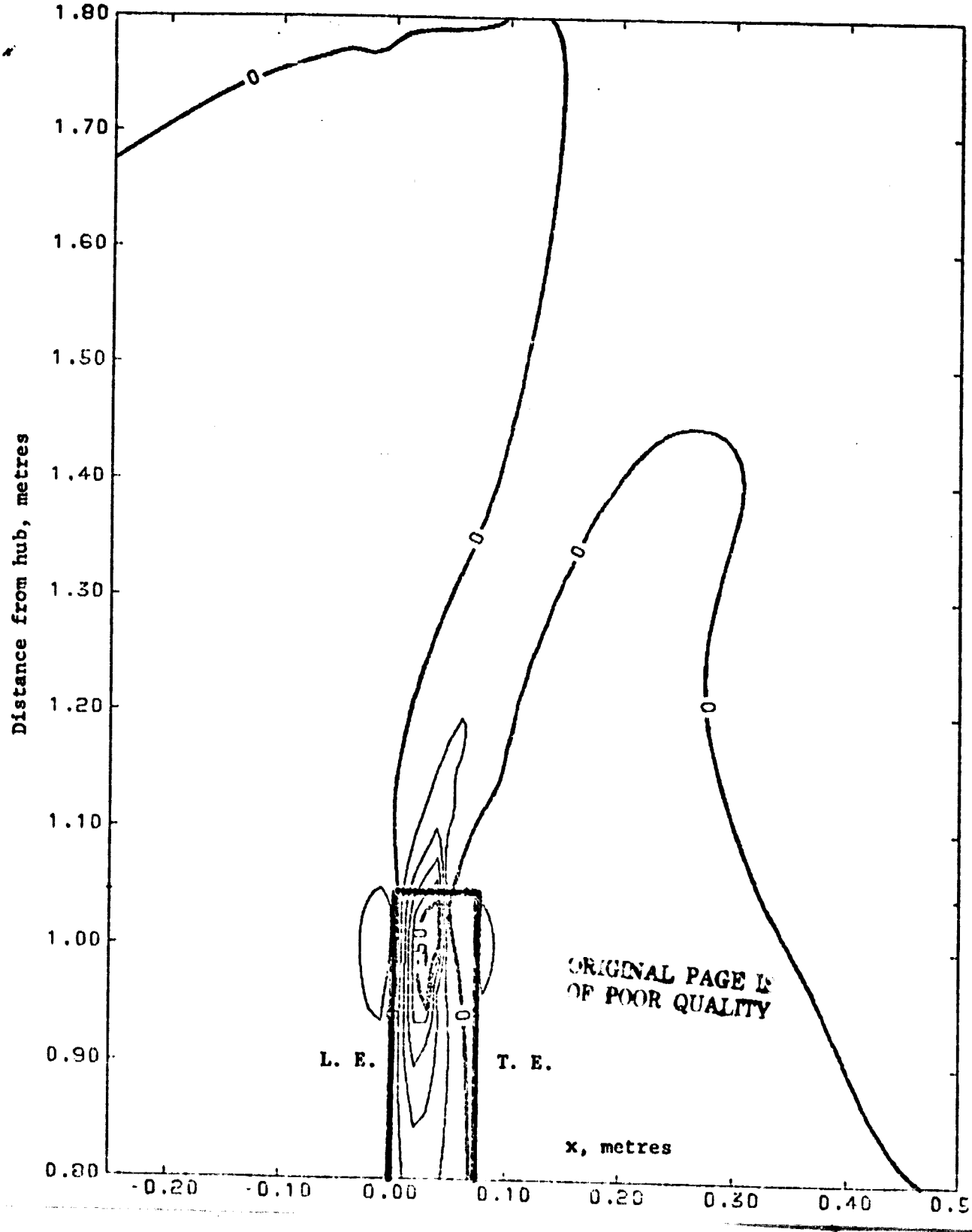

Figure 4.

$(n - n_o)$ FIELD IN PLANE 5.2 cm. ABOVE THE BLADE

contour interval = 4×10^{-6}

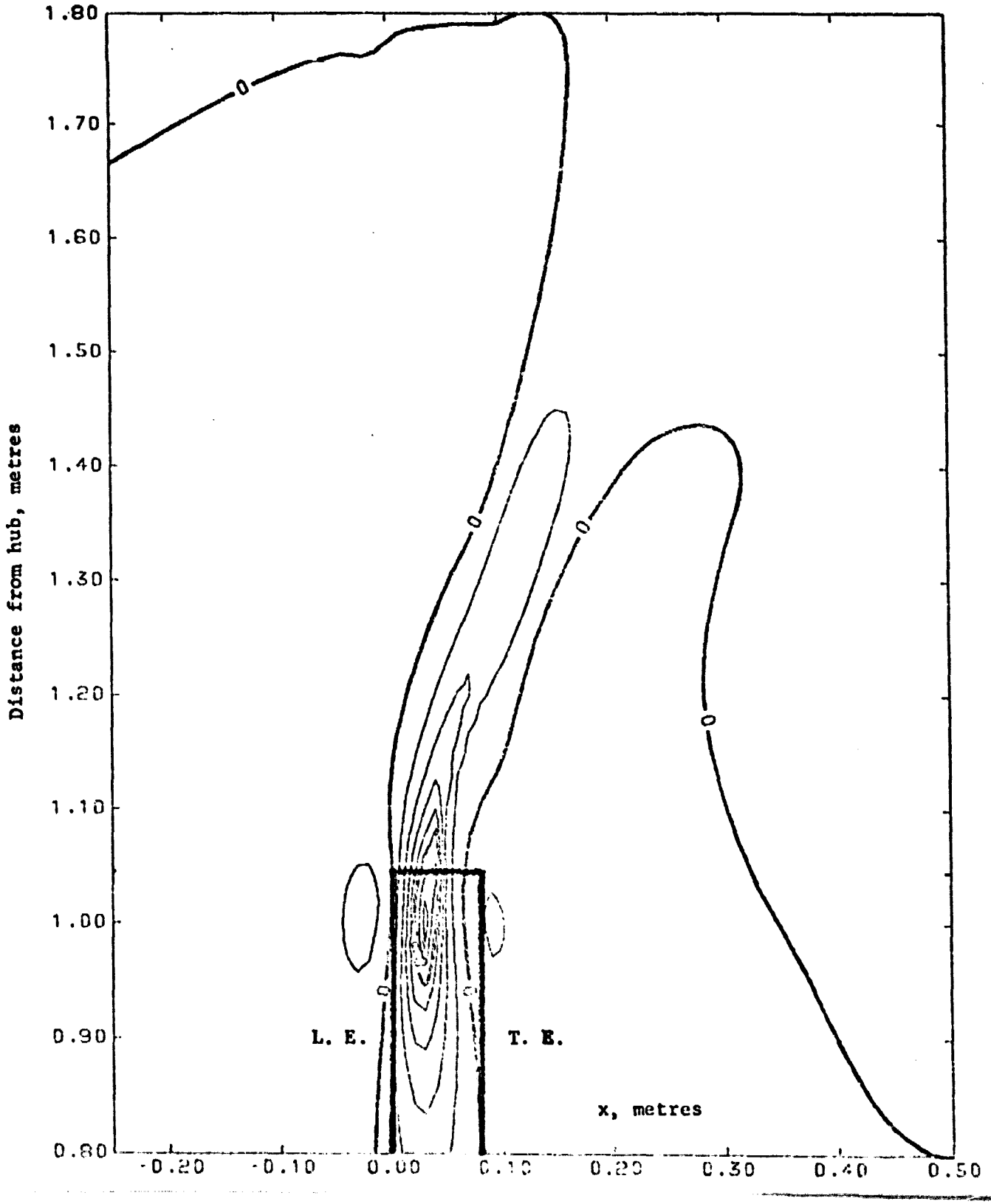

Figure 5.

$(n - n_o)$ FIELD IN PLANE 7.6 cm. ABOVE THE BLADE

contour interval = 2×10^{-6}

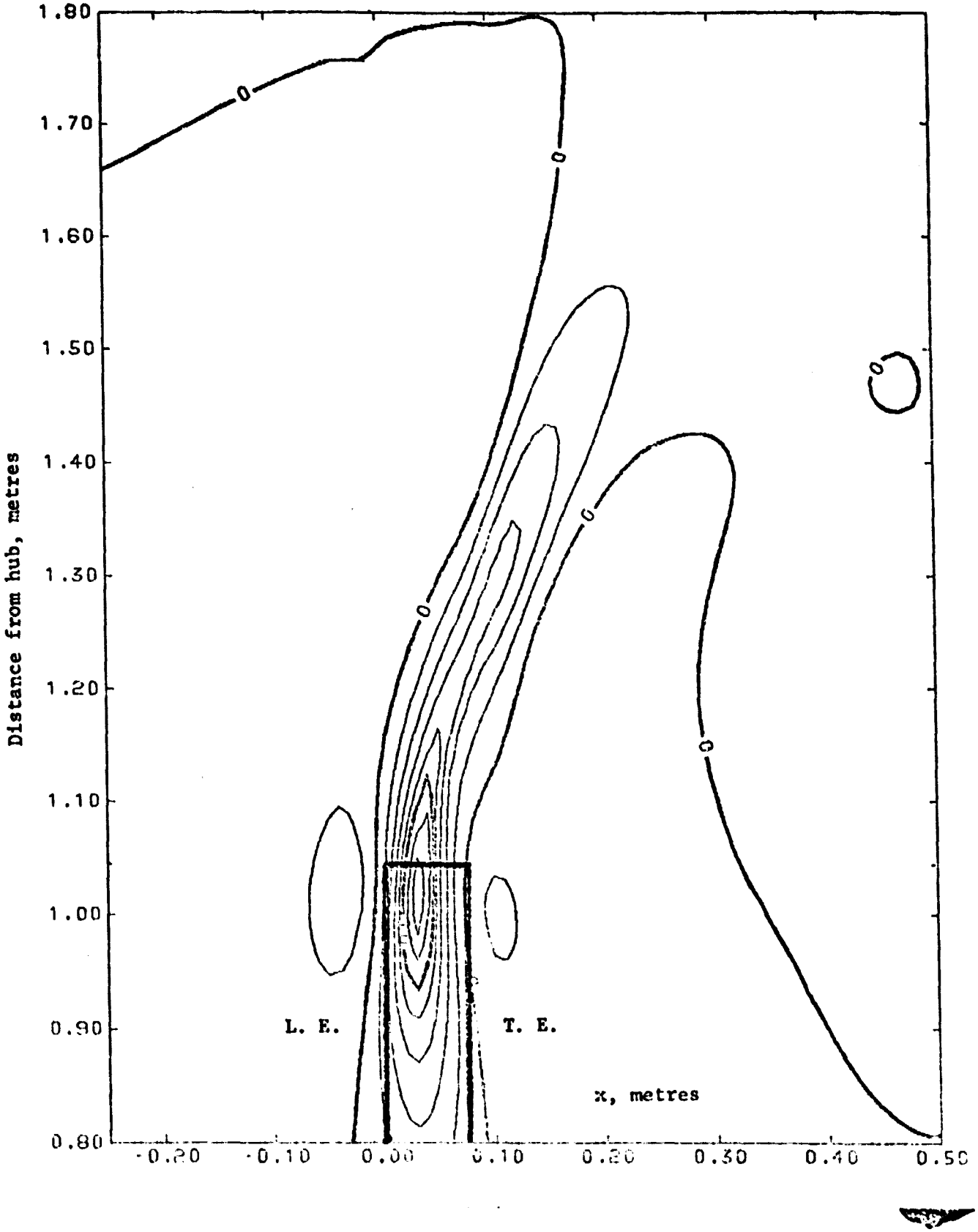

Figure 6.

$(n - n_o)$ FIELD IN PLANE 10.8 cm. ABOVE THE BLADE

contour interval = 1×10^{-6}

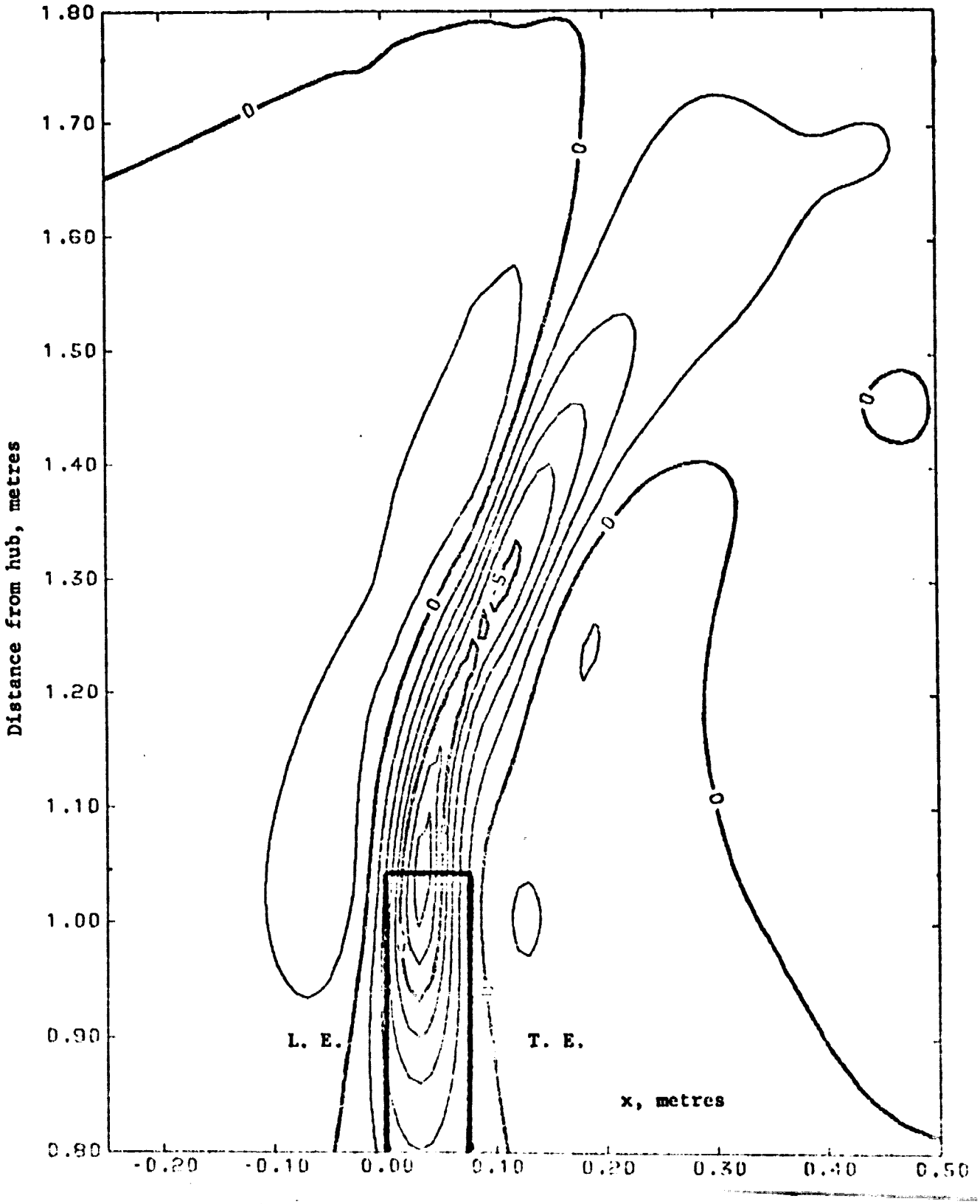

Figure 7.

$(n - n_o)$ FIELD IN PLANE 21.3 cm. ABOVE THE BLADE

contour interval = 0.4×10^{-6}

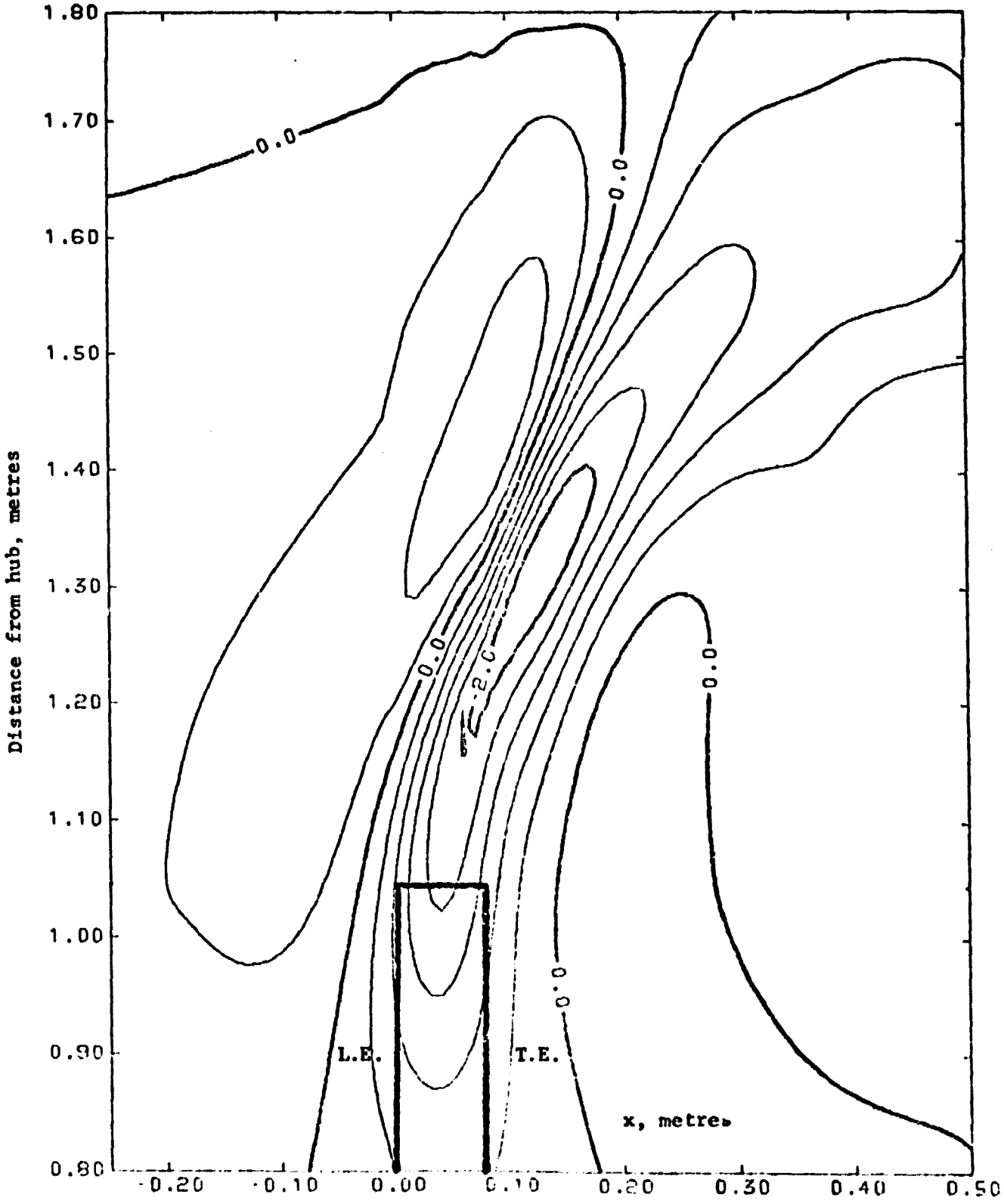

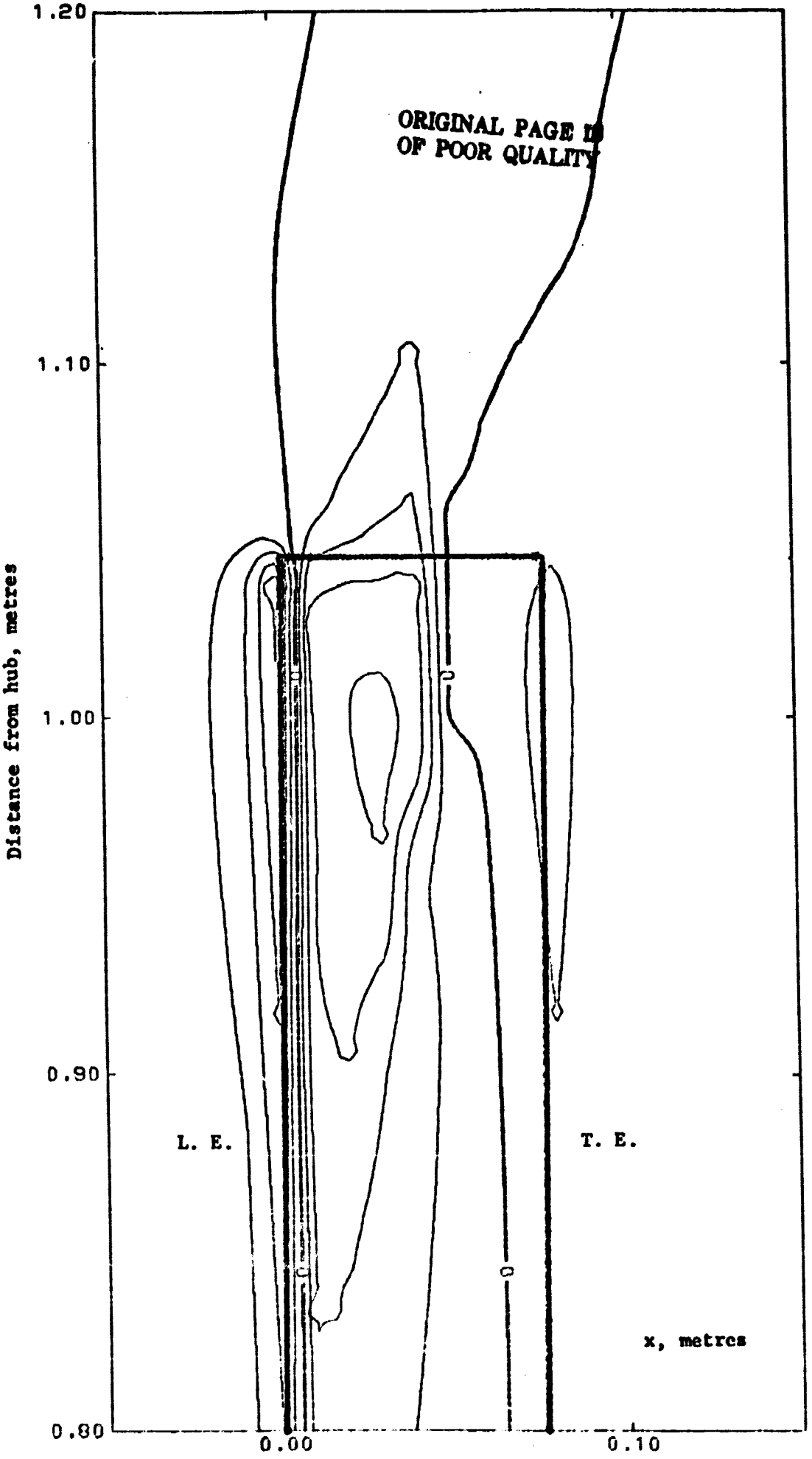

Figure 8. $(n - n_o)$ FIELD IN PLANE 0.11 cm. ABOVE THE BLADE
contour interval = 20×10^{-6}

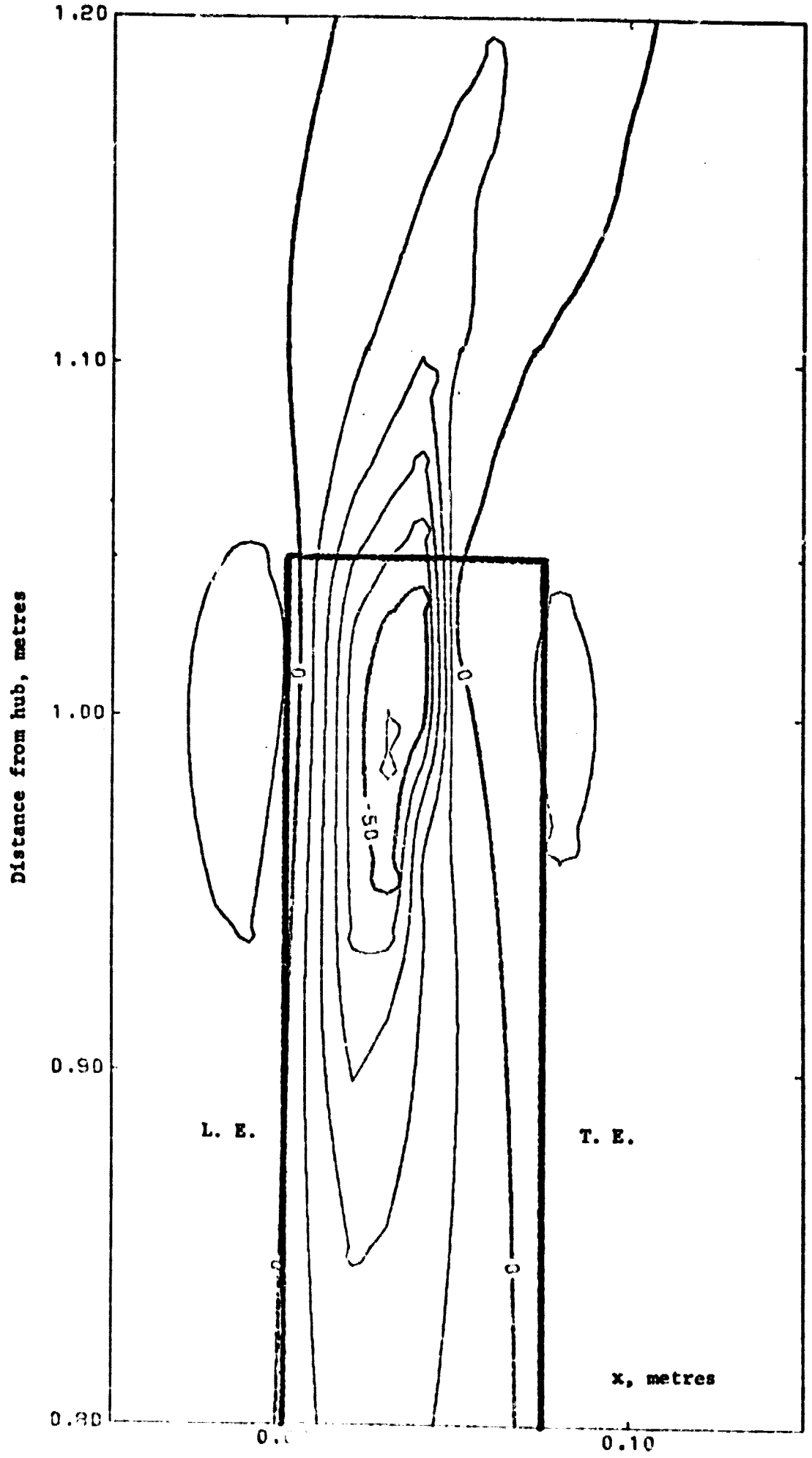

Figure 9. $(n - n_0)$ FIELD IN PLANE 2.2 cm. ABOVE THE BLADE
contour interval = 10×10^{-6}

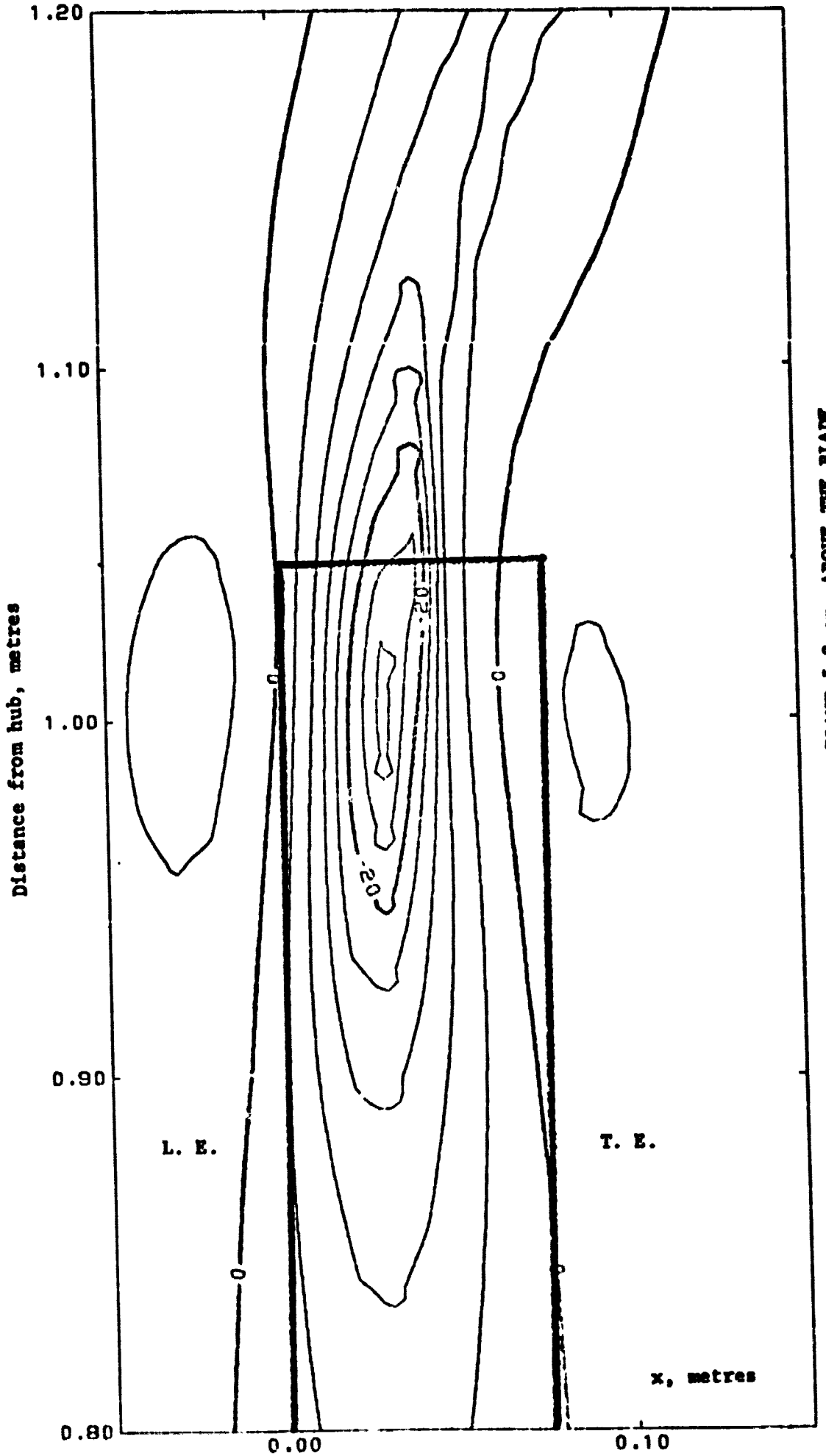

Figure 10. $(n - n_0)$ FIELD IN PLANE 5.2 cm. ABOVE THE BLADE
contour interval = 4×10^{-6}

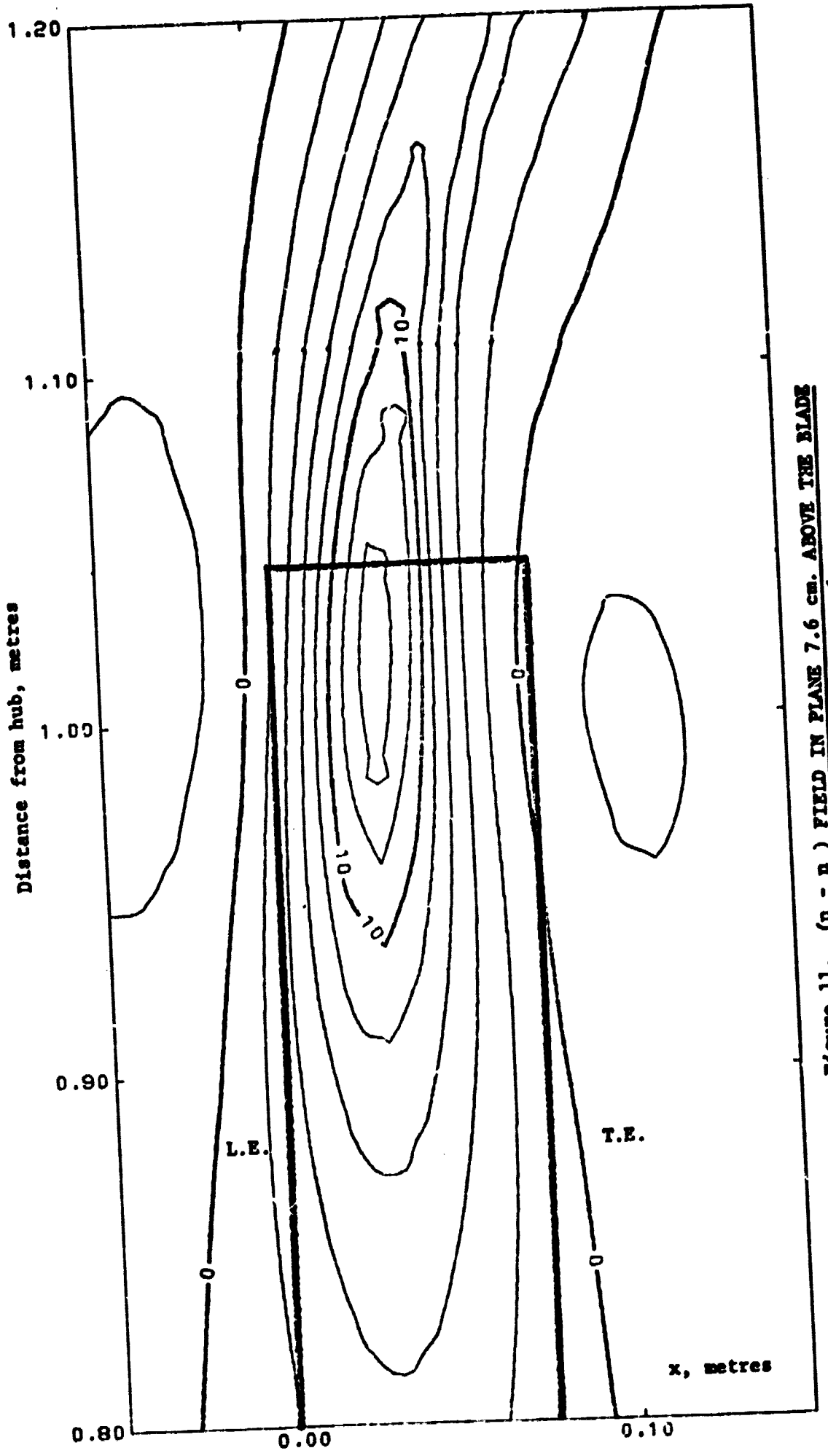

Figure 11. $(n - n_o)$ FIELD IN PLANE 7.6 cm. ABOVE THE BLADE
contour interval = 2×10^{-6}

Figure 13. CHORDWISE PROJECTION OF THE $(n - n_o)$ FIELD

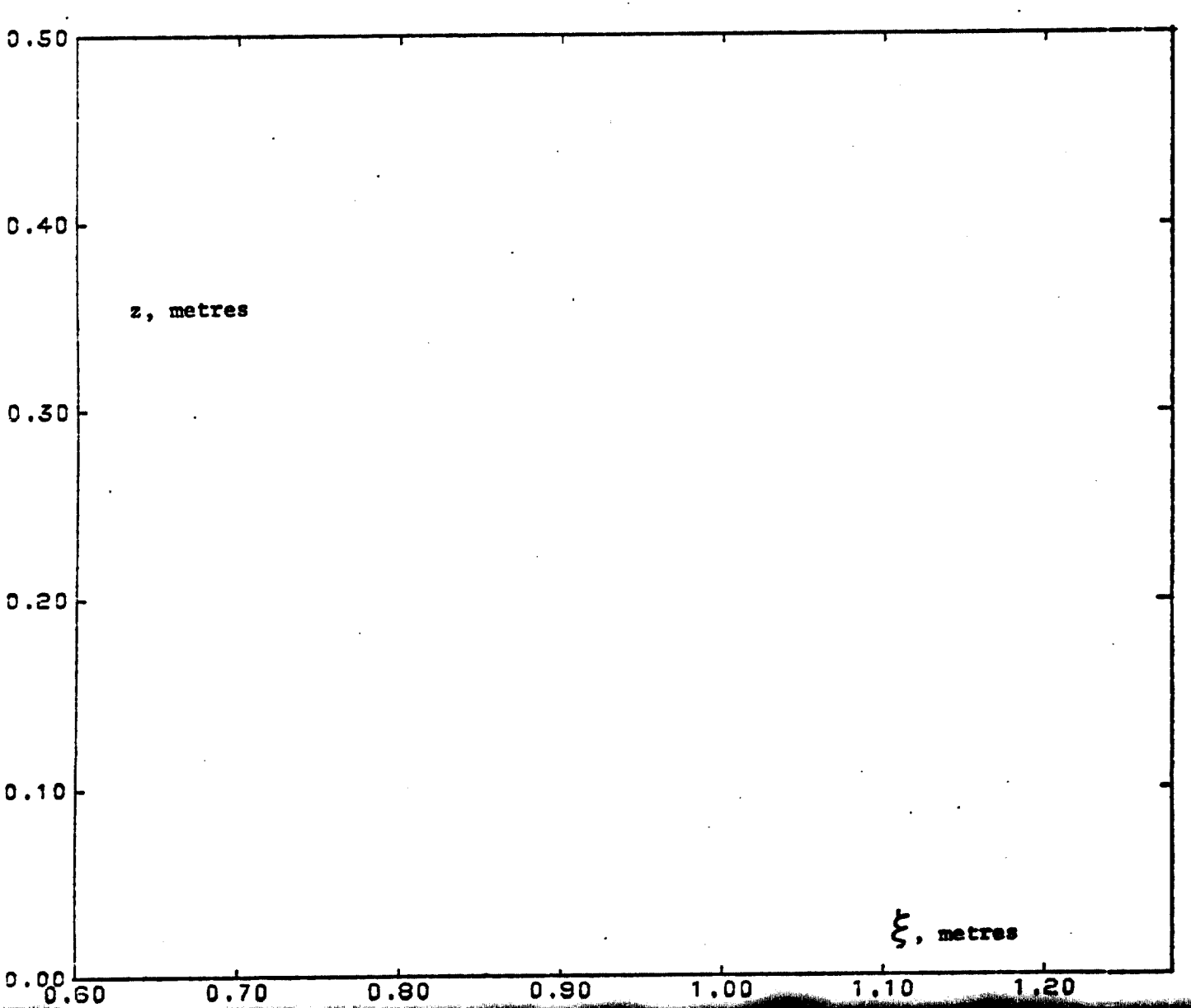

Figure 14. PROJECTION OF THE $(n - n_o)$ FIELD AT $+30^\circ$ FROM CHORDWISE

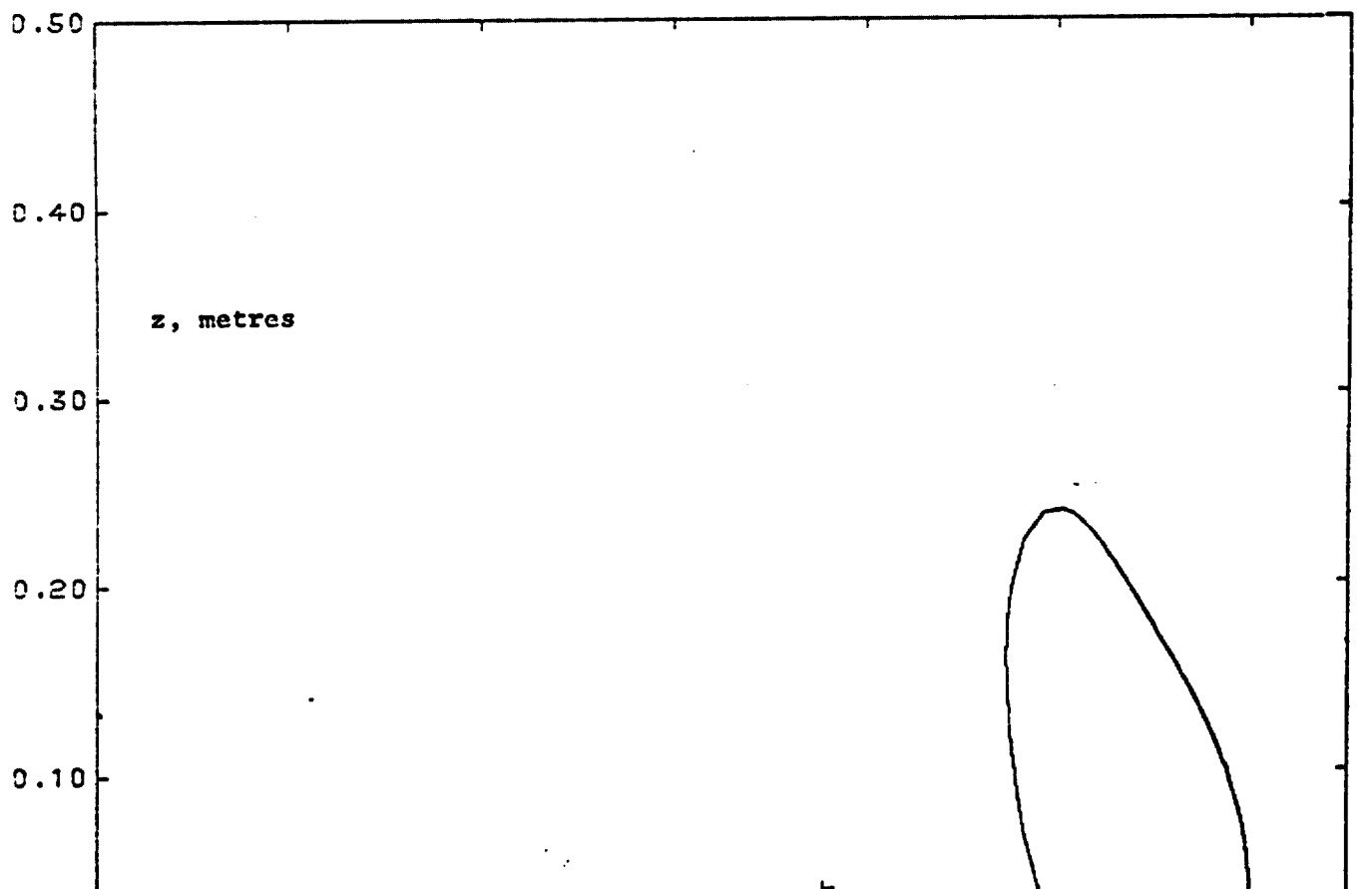

Figure 15. PROJECTION OF THE $(n - n_o)$ FIELD AT +45° FROM CHORDWISE

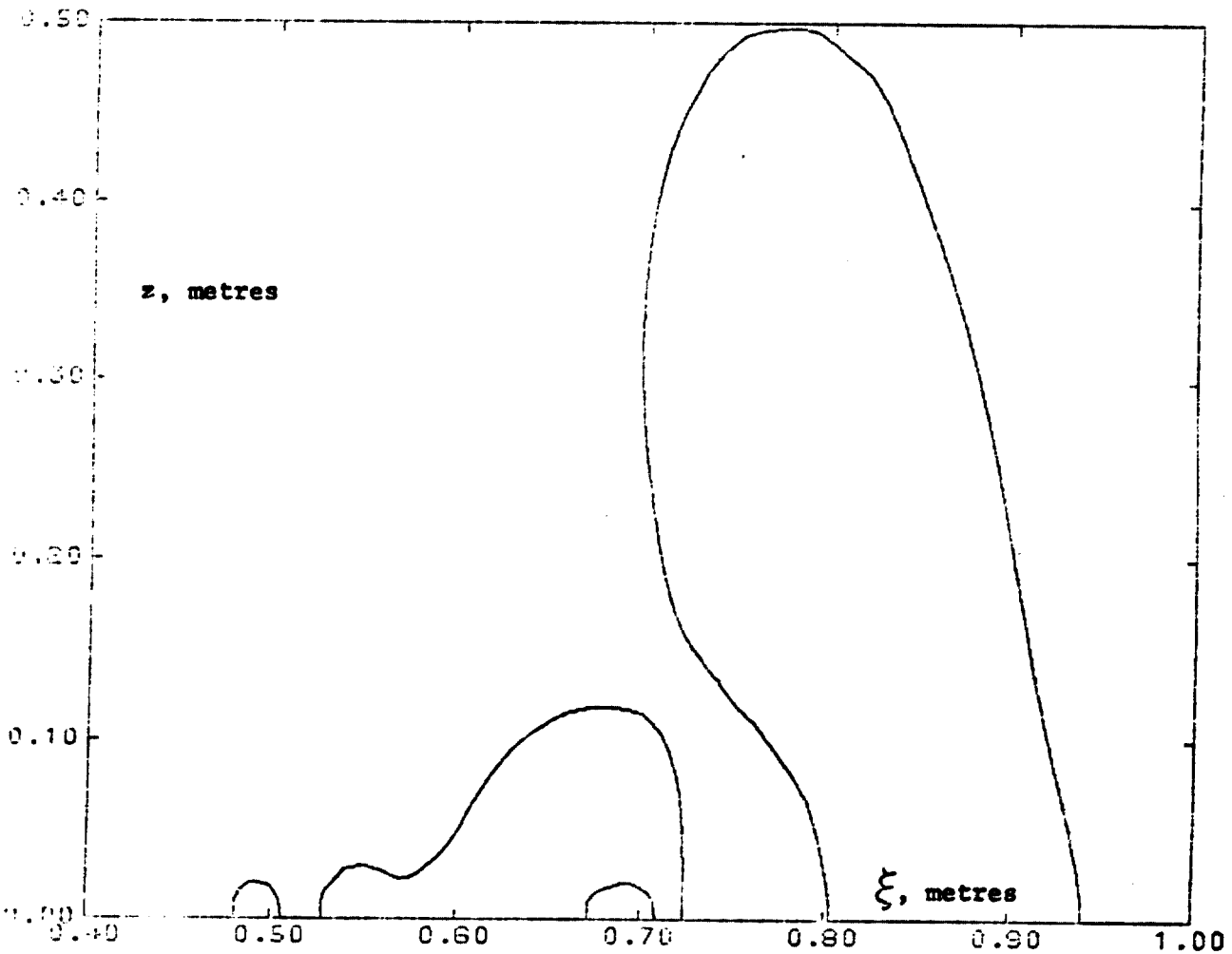

Figure 16. PROJECTION OF THE $(n - n_o)$ FIELD AT $+60^\circ$ FROM CHORDWISE

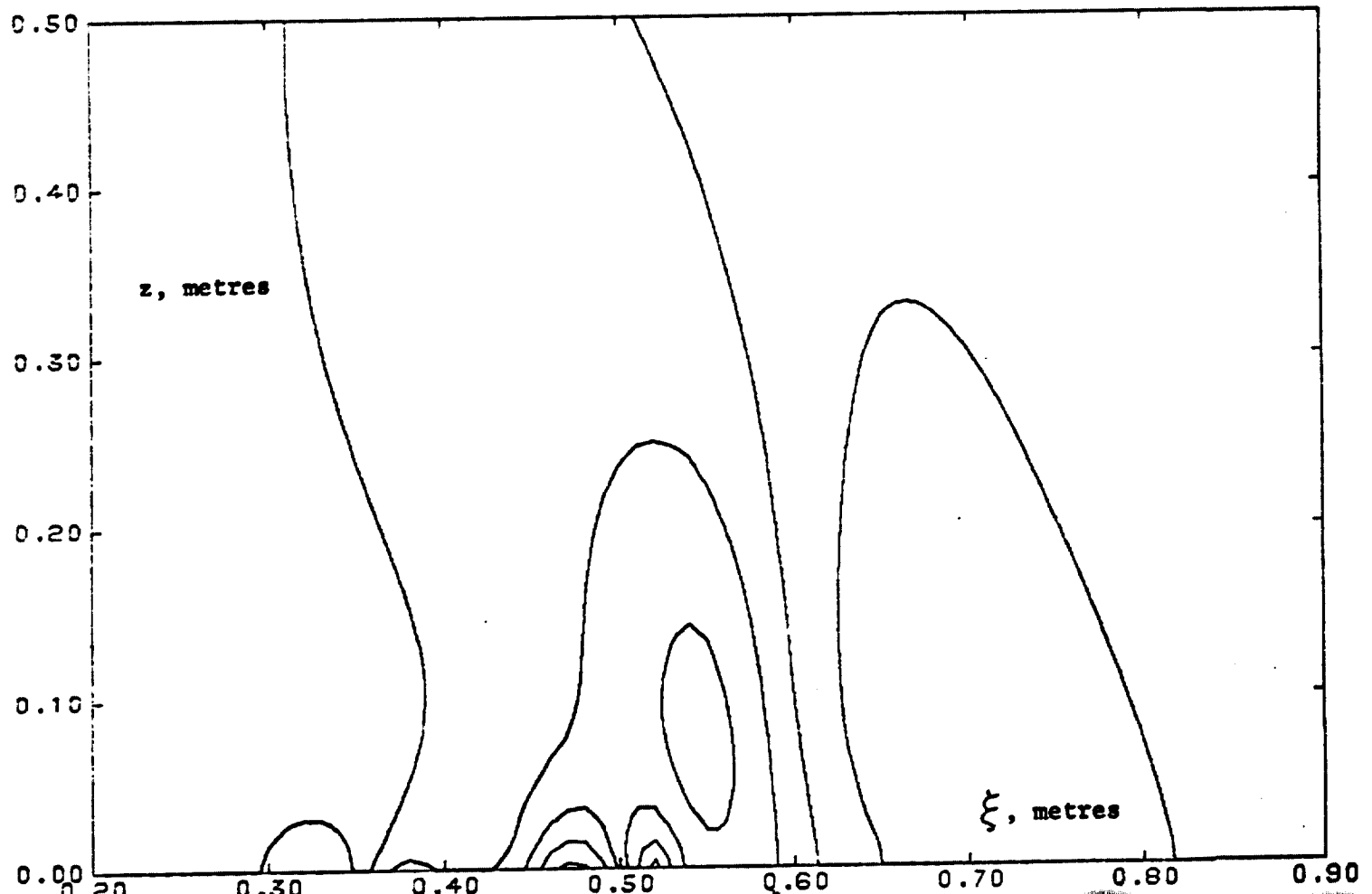

Figure 17. PROJECTION OF THE $(n - n_o)$ FIELD AT $+75^\circ$ FROM CHORDWISE

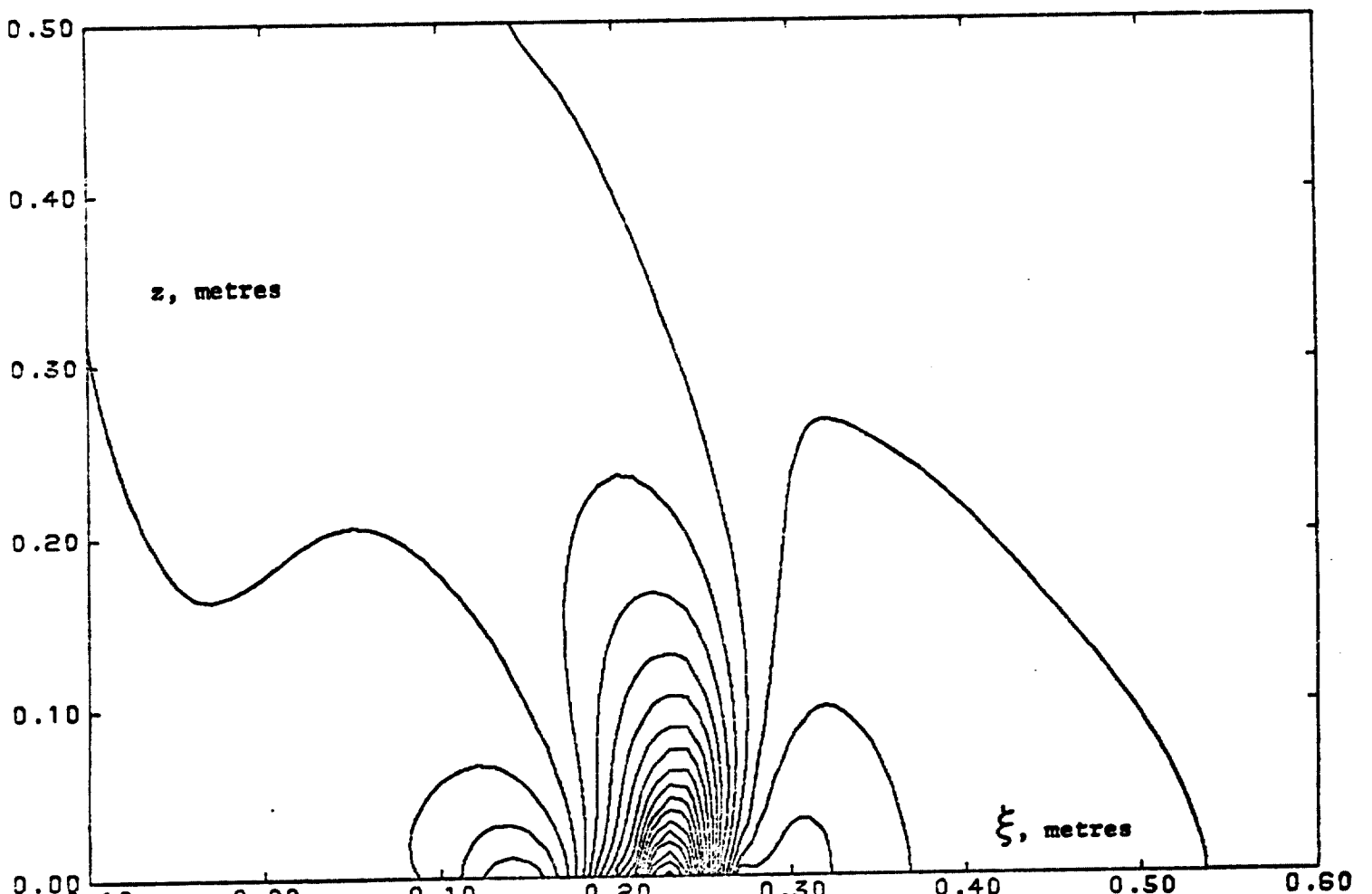

Figure 18. RADIAL PROJECTION OF THE $(n - n_o)$ FIELD

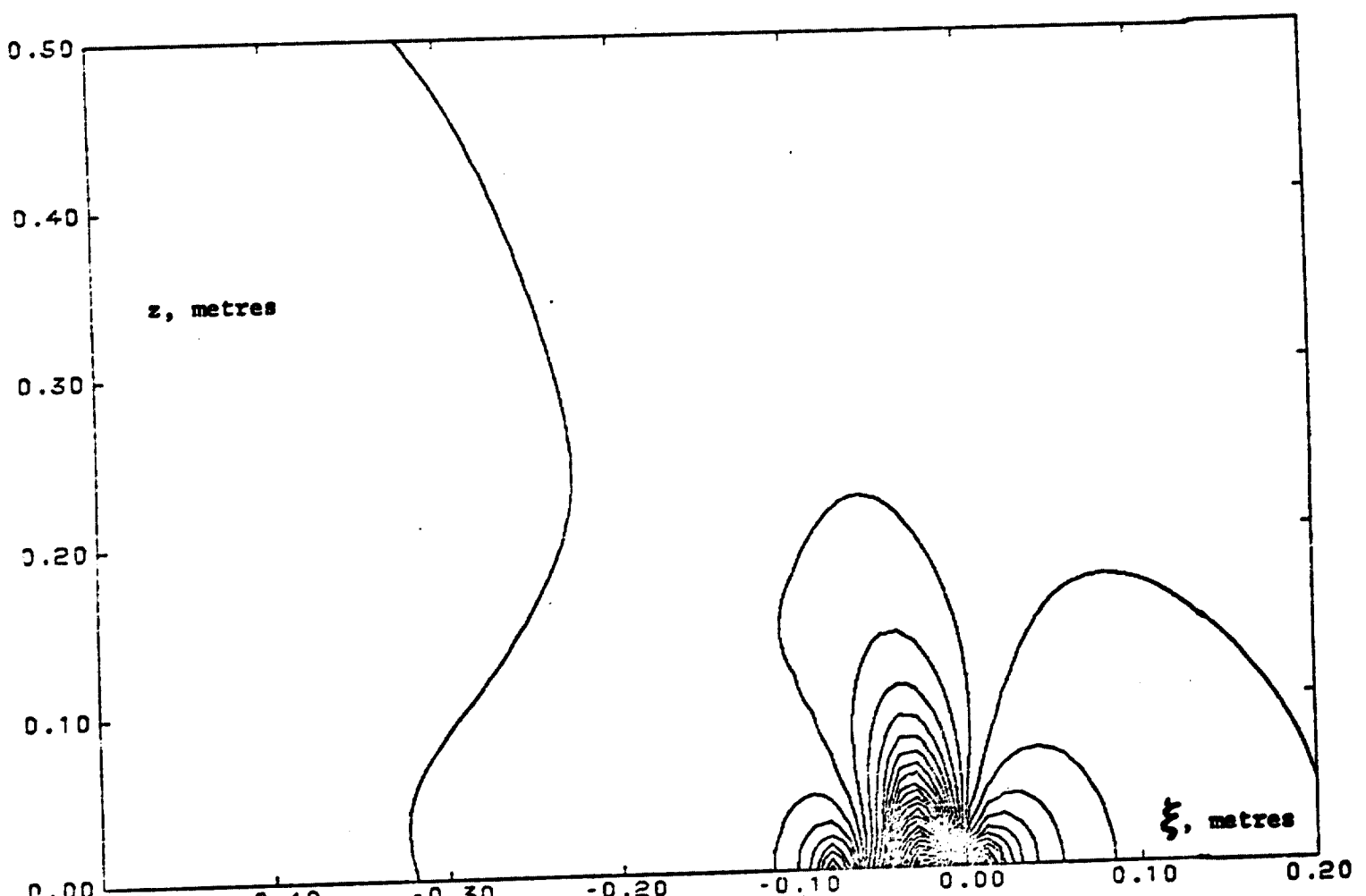

Figure 19. PROJECTION OF THE $(n - n_o)$ FIELD AT -75° FROM CHORDWISE

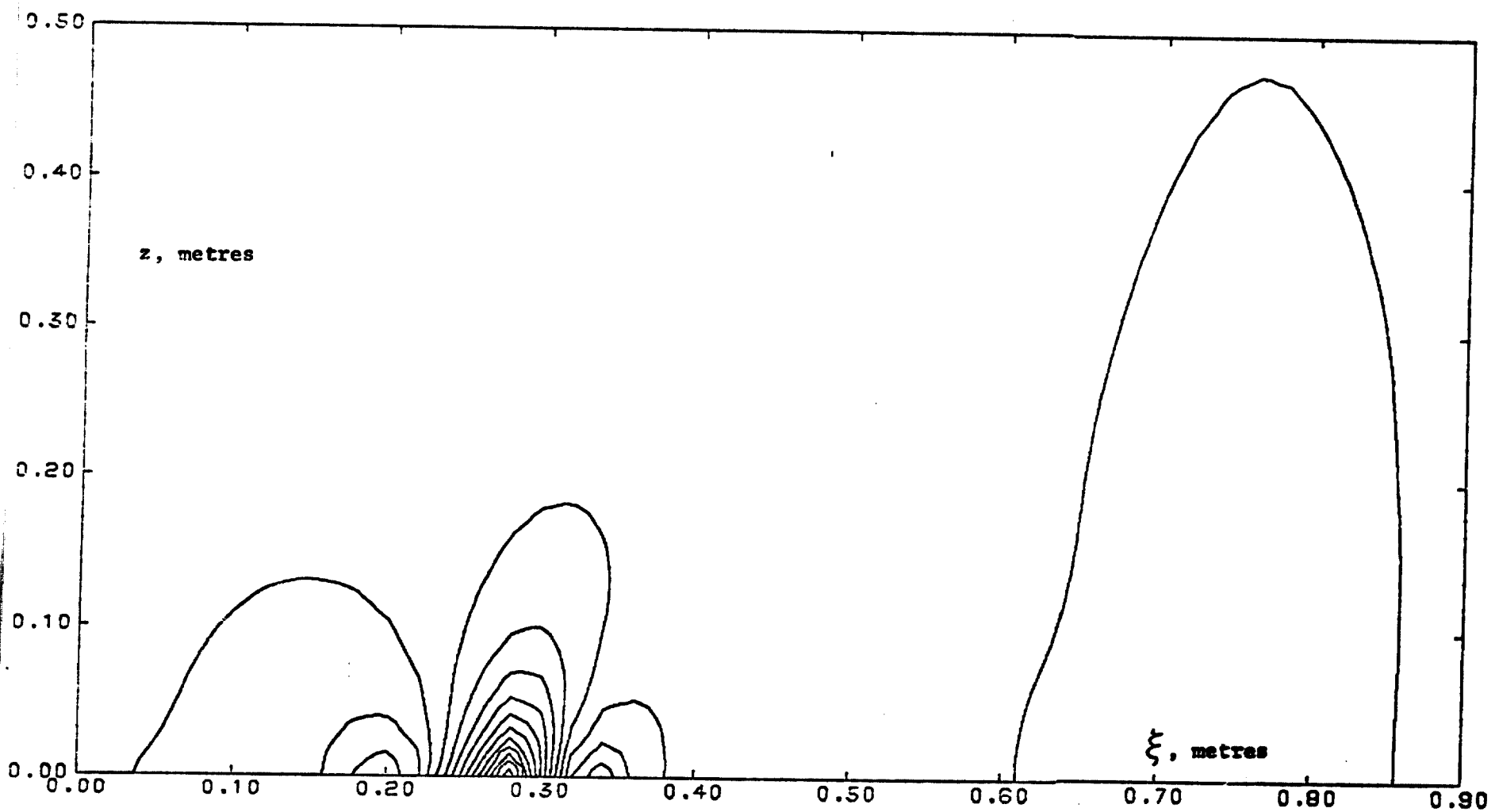

Figure 20. PROJECTION OF THE $(n - n_o)$ FIELD AT -60° FROM CHORDWISE

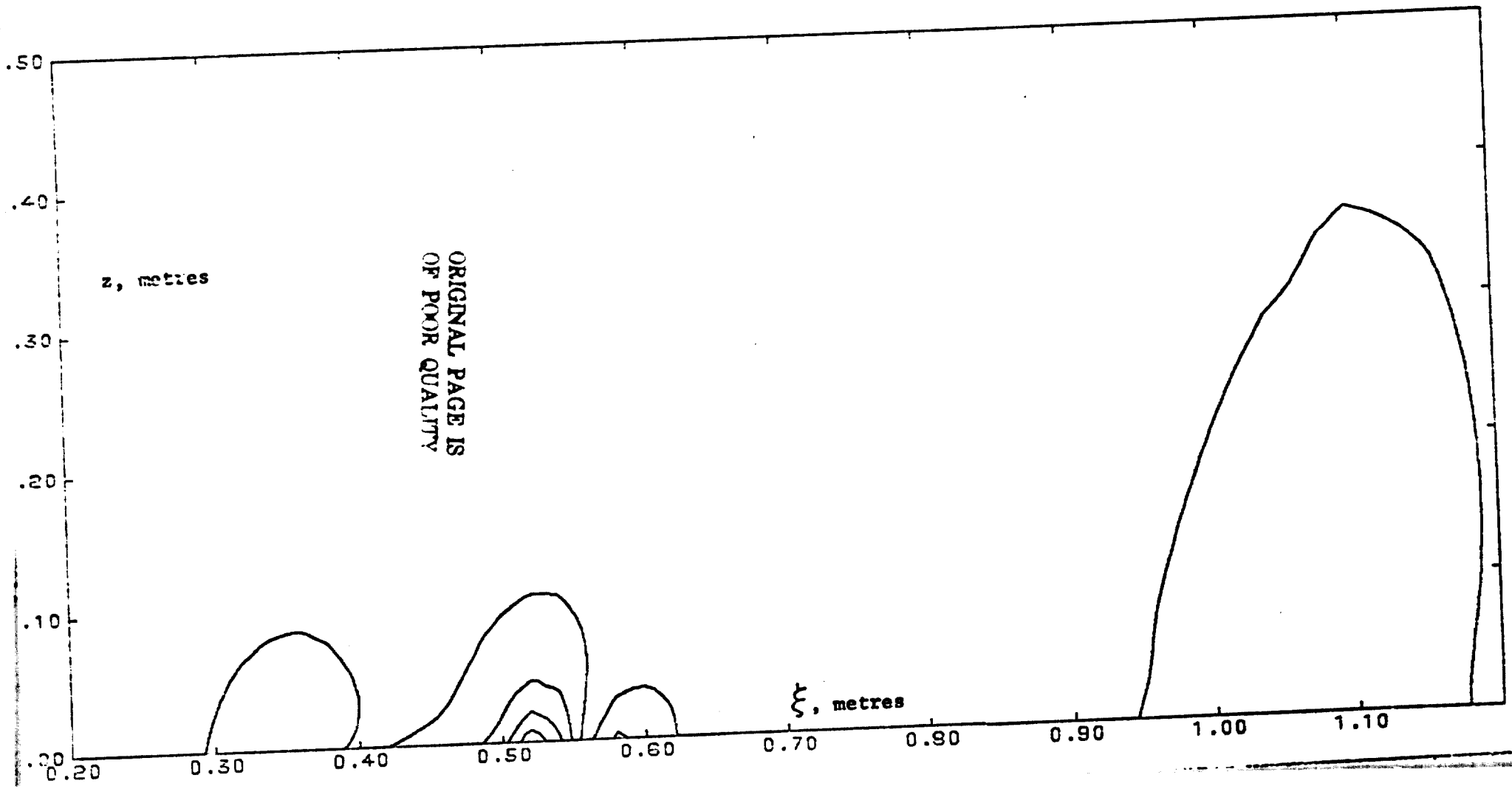

Figure 21. PROJECTION OF THE $(n - n_o)$ FIELD AT -45° FROM CHORDWISE

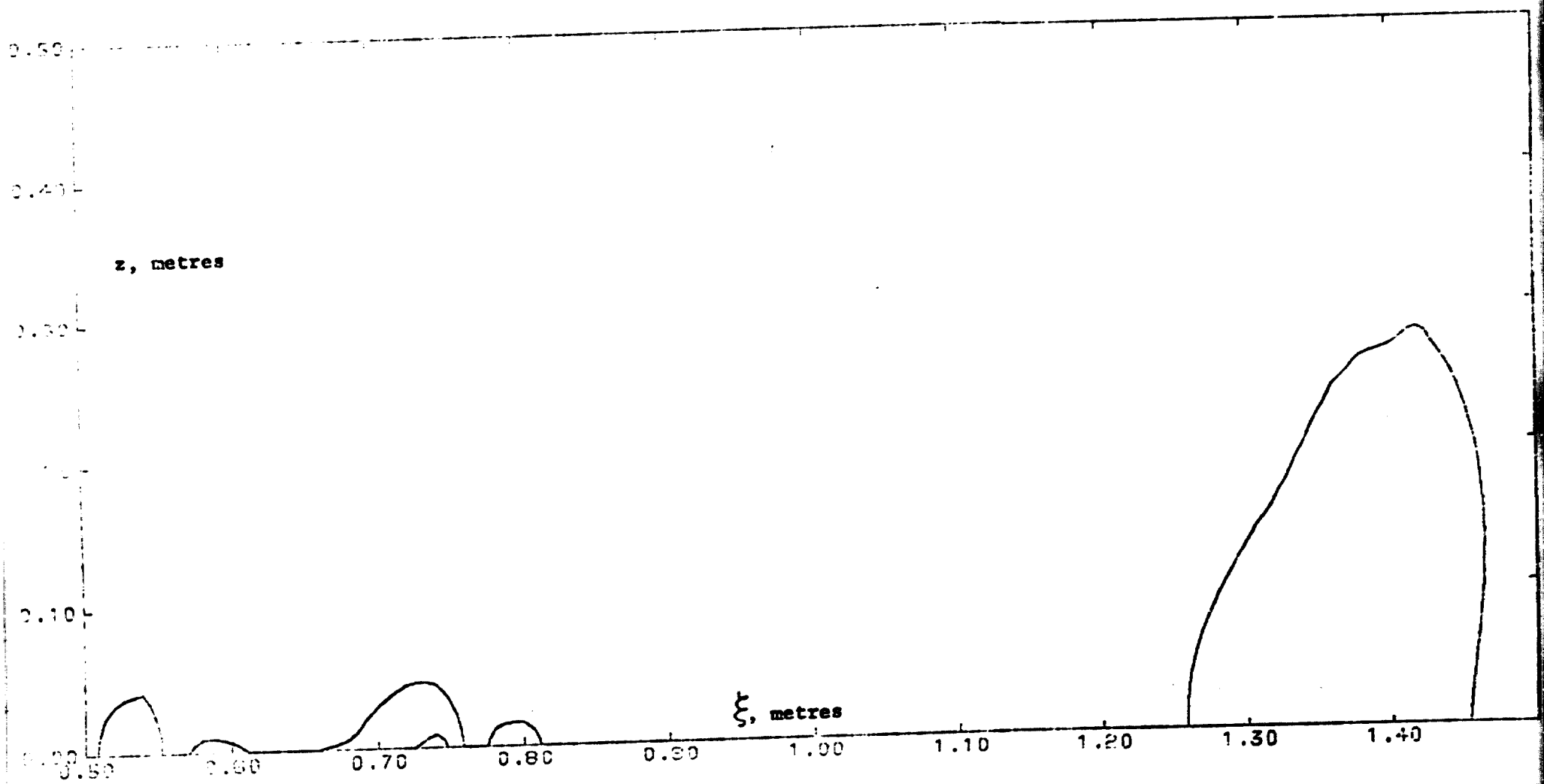

Figure 22. PROJECTION OF THE $(n - n_o)$ FIELD AT -30° FROM CHORDWISE